



HAL
open science

Molecular bases of an alternative dual-enzyme system for light color acclimation of marine *Synechococcus* cyanobacteria

Théophile Grébert, Adam A Nguyen, Suman Pokhrel, Kes Lynn, Morgane Ratin, Louison Dufour, Bo Chen, Allissa M Haney, Jonathan A Karty, Jonathan C Trinidad, et al.

► To cite this version:

Théophile Grébert, Adam A Nguyen, Suman Pokhrel, Kes Lynn, Morgane Ratin, et al.. Molecular bases of an alternative dual-enzyme system for light color acclimation of marine *Synechococcus* cyanobacteria. Proceedings of the National Academy of Sciences of the United States of America, 2021, 10.1073/pnas.2019715118. hal-03153666

HAL Id: hal-03153666

<https://hal.science/hal-03153666>

Submitted on 26 Feb 2021

HAL is a multi-disciplinary open access archive for the deposit and dissemination of scientific research documents, whether they are published or not. The documents may come from teaching and research institutions in France or abroad, or from public or private research centers.

L'archive ouverte pluridisciplinaire **HAL**, est destinée au dépôt et à la diffusion de documents scientifiques de niveau recherche, publiés ou non, émanant des établissements d'enseignement et de recherche français ou étrangers, des laboratoires publics ou privés.

1 **Molecular bases of an alternative dual-enzyme system for light color**
2 **acclimation of marine *Synechococcus* cyanobacteria**

3
4 Théophile Grébert^{a,§,1}, Adam A. Nguyen^{b,c,1}, Suman Pokhrel^b, Kes Lynn Joseph^b, Morgane Ratin^a, Louison
5 Dufour^a, Bo Chen^d, Allissa M. Haney^d, Jonathan A. Karty^e, Jonathan C. Trinidad^e, Laurence Garczarek^a, Wendy
6 M. Schluchter^b, David M. Kehoe^d and Frédéric Partensky^{a,*}

7 ^aSorbonne Université & CNRS, UMR 7144, Ecology of Marine Plankton (ECOMAP) Team, Station Biologique,
8 29688 Roscoff, France; ^bDepartment of Biological Sciences, University of New Orleans, New Orleans, LA
9 70148, USA; ^cDepartment of Chemistry, University of New Orleans, New Orleans, LA 70148, USA;
10 ^dDepartment of Biology, Indiana University, Bloomington, IN 47405, USA; ^eDepartment of Chemistry,
11 Indiana University, Bloomington, Indiana 47405, USA

12 [§]Present address: Pasteur Institute, Department of Microbiology, Synthetic Biology Group, 75015 Paris,
13 France

14 *To whom correspondence may be addressed. Email: frederic.partensky@sb-roscoff.fr.

15

16 **Keywords:** light regulation; marine cyanobacteria; photosynthesis; phycobilin lyase; phycoerythrin

17 **Abbreviations :** BL, blue light; CA4, Type IV chromatic acclimation; EICs, extracted ion chromatograms; GL,
18 green light; HT-, hexahistidine-tagged; LC, liquid chromatography; MS, mass spectrometry; MS/MS, tandem
19 mass spectrometry; MW, molecular weight; PBS, phycobilisome; PC, phycocyanin; PCB, phycocyanobilin;
20 PEB, phycoerythrobin; PEI, phycoerythrin-I; PEII, phycoerythrin-II; PT, pigment type; PUB, phycourobilin

¹ T.G and A.A.N. contributed equally to this work.

21 **Abstract**

22 Marine *Synechococcus* cyanobacteria owe their ubiquity in part to the wide pigment diversity of their light-
23 harvesting complexes. In open ocean waters, cells predominantly possess sophisticated antennae with rods
24 composed of phycocyanin and two types of phycoerythrins (PEI and PEII). Some strains are specialized for
25 harvesting either green or blue light, while others can dynamically modify their light absorption spectrum to
26 match the dominant ambient color. This process called 'Type-IV chromatic acclimation' (CA4) has been linked
27 to the presence of a small genomic island occurring in two configurations (CA4-A and -B). While the CA4-A
28 process has been partially characterized, the CA4-B process has remained an enigma. Here, we characterize
29 the function of two members of the phycobilin lyase E/F clan, MpeW and MpeQ, in *Synechococcus* sp. strain
30 A15-62 and demonstrate their critical role in CA4-B. While MpeW, encoded in the CA4-B island and
31 upregulated in green light, attaches the green-light absorbing chromophore phycoerythrobilin to cysteine-83
32 of the PEII α -subunit in green light, MpeQ binds phycoerythrobilin and isomerizes it into the blue-light
33 absorbing phycourobilin at the same site in blue light, reversing the relationship of MpeZ and MpeY in the
34 CA4-A strain RS9916. Our data thus reveal key molecular differences between the two types of chromatic
35 acclimators, both highly abundant but occupying distinct complementary ecological niches in the ocean. They
36 also support an evolutionary scenario whereby CA4-B island acquisition allowed former blue-light specialists
37 to become chromatic acclimators, while former green-light specialists would have acquired this capacity by
38 gaining a CA4-A island.

39

40 **Significance**

41 Of all cyanobacteria on Earth, marine *Synechococcus* are those displaying the greatest pigment diversity. The
42 most sophisticated pigment type are cells able to reversibly modify their color by a phenomenon called Type

43 IV chromatic acclimation or CA4. Two genetically distinct CA4 types (CA4-A and CA4-B) have evolved in
44 different lineages. Together, they represent almost half of all *Synechococcus* cells in oceanic areas, and are
45 equally abundant but occupy complementary ecological niches. While the molecular mechanism of CA4-A
46 has recently started to be deciphered, the CA4-B mechanism was so far uncharacterized. Here, by unveiling
47 this mechanism and demonstrating its singularity relative to CA4-A, we provide novel highlights on the
48 evolutionary history of *Synechococcus* acclimation to light color in the oceans.

49

50 \body

51 **Introduction**

52 Marine *Synechococcus* are the second most abundant phototrophs in the oceans, significantly contributing
53 to oceanic primary production and carbon cycling (1, 2). These picocyanobacteria occupy the upper lit layer
54 of marine waters from the equator up to 80 °N (3, 4) and exhibit a broad range of photosynthetic pigments,
55 allowing them to optimally exploit a large variety of light environments, from particle-loaded estuaries to
56 the optically clear open ocean waters (5). This pigment diversity arises from a large flexibility in the
57 composition of their light-harvesting antennae, called phycobilisomes (PBS). Structurally, these complexes
58 comprise a central core from which radiate six or eight rods made of α/β heterodimers of phycobiliproteins
59 that first assemble into $(\alpha\beta)_6$ hexamers and then stack into rods with the assistance of linker proteins (6). In
60 the open ocean, virtually all *Synechococcus* cells belong to pigment type 3 (PT 3), in which PBS rods are made
61 of the three phycobiliproteins, phycocyanin (PC), phycoerythrin-I (PEI) and phycoerythrin-II (PEII), which can
62 covalently bind three chromophore types: the red-light absorbing phycocyanobilin (PCB, $A_{\max} = 650\text{nm}$), the
63 green-light (GL) absorbing phycoerythrobilin (PEB, $A_{\max} = 550\text{ nm}$) and the blue-light (BL) absorbing
64 phycourobilin [PUB, $A_{\max} = 495\text{ nm}$ (7, 8)]. Different pigment subtypes have been defined within PT 3, based

65 on the relative ratio of fluorescence excitation at 495 nm and 545 nm with emission at 580 nm ($\text{Exc}_{495:545}$), a
66 proxy for their molar PUB:PEB ratio. This ratio is constitutively low ($\text{Exc}_{495:545} < 0.6$), intermediate
67 ($0.6 \leq \text{Exc}_{495:545} < 1.6$) or high ($\text{Exc}_{495:545} \geq 1.6$) in PT 3a, 3b and 3c, respectively (5, 9). Furthermore, in PT 3d
68 strains, which appear to make up nearly half of the PT 3 population globally (9), the PUB:PEB ratio can
69 reversibly vary with ambient light color, a process called type IV chromatic acclimation (CA4) that allows cells
70 to optimally absorb either GL or BL, depending on the ambient ratio of these light colors (10, 11). While most
71 genes coding for PBS rod components are localized in a large genomic region, called the PBS region (5), strains
72 capable of CA4 additionally possess a small genomic island existing in one of two distinct configurations (12).
73 Each contains the two regulators encoded by *fciA* and *fciB* (13) and one gene coding for a putative phycobilin
74 lyase family member, which can be either *mpeZ* or *mpeW*, defining the two distinct genotypes CA4-A and
75 CA4-B [the corresponding PTs are named 3dA and 3dB, respectively; (12)]. Phycobilin lyases are enzymes
76 responsible for the covalent attachment of chromophores at specific cysteine residues of phycobiliprotein
77 subunits and are thus key players in *Synechococcus* pigmentation. Indeed, chromophore ligation takes place
78 prior to phycobiliprotein subunit assembly, and proper phycobilin arrangement is crucial for efficient energy
79 transfer along the rods (14). However, among the dozen (putative) phycobilin lyases encoded in marine
80 *Synechococcus* genomes (5), only a few have been biochemically characterized. RpeG from *Synechococcus*
81 sp. WH8102 (PT 3c) was shown to attach PEB to cysteine-84 (C84) of the α -subunit of PC and to isomerize it
82 to PUB (15). Such dual-function enzymes are called phycobilin lyase-isomerases. More recently, the
83 biochemical characterization of the CA4-A strain *Synechococcus* sp. RS9916 (clade IX) revealed the specific
84 chromophore changes that occur during CA4, namely one out of five chromophore-binding sites on PEI and
85 two of the six sites of PEII change from PEB in GL to PUB in BL. Two enzymes implicated in CA4-A and
86 belonging to the E/F structural clan (16) have been characterized: MpeZ is the lyase-isomerase adding PUB
87 at C83 of the PEII α -subunit (MpeA) in BL (17), whereas its paralog MpeY is the PEB lyase acting on the same
88 site in GL (18). While *mpeZ* was found to be expressed more highly under BL (12, 13, 17), *mpeY* is

89 constitutively expressed whatever the ambient light color. This led to the suggestion that the cellular
90 MpeZ:MpeY protein ratio ultimately controls the chromophore bound at MpeA-C83 (18). By contrast, the
91 identity and function of the corresponding enzymes in CA4-B strains was so far unknown.

92 Here, we characterize the *mpeW* gene located in the CA4 genomic island of the CA4-B strain
93 *Synechococcus* sp. A15-62 (sub-clade IIc). We show that it encodes a phycobilin lyase acting on MpeA-C83 in
94 GL that vies a previously unidentified lyase-isomerase (MpeQ) acting on the same cysteine position in BL.
95 Our results highlight the key role of the diversification of the MpeY enzyme family in the adaptation of marine
96 *Synechococcus* to different light color niches and provide new insights to explain the occurrence of two
97 mutually exclusive CA4 systems in marine *Synechococcus*.

98

99 Results

100 **The MpeY Phycobilin Lyase Family Is Polyphyletic.** Based on its conserved genomic position in the PEII-
101 specific sub-region of the PBS region (Fig. 1A) and on sequence similarity, the gene located immediately
102 upstream of the *mpeBA* operon (encoding the two subunits of PEII) was previously named *mpeY* in all
103 *Synechococcus* strains containing PEII (5, 9, 18). However, the phylogenetic analysis of the different members
104 of this family revealed that *mpeY* is in fact polyphyletic, with three distinct clusters, each corresponding to a
105 different pigment subtype (Fig. 1C). PT 3a strains (i.e., GL specialists) possess the MpeY^{3a} variant encoded by
106 the PT 3a-specific *mpeY* allele, PT 3dA strains contain the MpeY^{3dA} variant recently characterized in the PT
107 3dA strain *Synechococcus* sp. RS9916 as a PEB lyase acting on C83 of the α -PEII subunit (MpeA) (18), while a
108 third variant is found in PT 3c (i.e., BL specialists) and 3dB strains. Strikingly, sequences from the latter two
109 pigment sub-types were intermingled in the phylogenetic tree, as was previously observed for *mpeBA* or
110 *cpeBA* phylogenies, indicating that PBS genes of these pigment subtypes are phylogenetically too close to be
111 distinguishable (9, 12). Tandem mass spectrometry analysis of the chromophorylation of MpeA from the PT

112 3a strain *Synechococcus* sp. WH7803 revealed that MpeA-C83 binds a PEB, while PUB is bound to both MpeA-
113 C75 and 140 (*SI Appendix*, Fig. S1). This suggests that MpeY^{3a} must have a PEB lyase function, like MpeY^{3dA}.
114 In contrast, as demonstrated below, the function of the MpeY-like protein found in PT 3c and 3dB differs
115 from that of both MpeY^{3a} and MpeY^{3dA} and we therefore renamed it 'MpeQ' in the tree (Fig. 1C) and in the
116 text hereafter. The protein sequences of MpeW, MpeZ, MpeQ, MpeY^{3a} and MpeY^{3dA} have on average 34-58%
117 amino acid identity over their whole length, compared to an average of 70-82% identity amongst members
118 of each of these sub-families (Fig. 1B and Dataset S1).

119
120 Chromophore Changes Occurring During CA4-B Are the Same as Those Occurring in the CA4-A Process.

121 Although the Exc_{495:545} ratios of CA4-A and -B strains have previously been shown to be similar in both BL
122 (1.6-1.7) and GL (0.6-0.7) (12), it was unclear what specific changes in chromophorylation were taking place
123 during the CA4 process in CA4-B strains. To investigate this, PBS from wild-type *Synechococcus* sp. A15-62
124 grown under BL or GL were purified, and PEI and PEII subunits separated by HPLC. Absorption spectra of
125 individual subunits (Fig. 2 and *SI Appendix*, Fig. S2) suggested that the PUB:PEB molar ratio changed between
126 GL and BL from 0:2 to 1:1 for the α -PEI subunit (CpeA) and from 1:2 to 3:0 for the α -PEII subunit (MpeA),
127 while the chromophorylation of β -PEI (CpeB) and β -PEII (MpeB) subunits did not vary with light color (1:2 in
128 both conditions; Table 1). The chromophorylation of the two α -subunits was further characterized by tandem
129 mass spectrometry, confirming the abovementioned molar ratios and demonstrating that the three cysteine
130 positions that change chromophorylation (from PEB in GL to PUB in BL) are MpeA-C83 and C140 and CpeA-
131 C139 (Table 1, Dataset S2 and *SI Appendix*, Figs. S3-S5), i.e. the same chromophores and positions as in the
132 CA4-A strain RS9916 (17).

133

134 **MpeW and MpeQ Are Required for PEB and PUB Attachment on MpeA, Respectively.** Since the biochemical
135 characterization of MpeZ and MpeY^{3dA} in RS9916 showed that they were respectively a PEB lyase-isomerase
136 and a PEB lyase, both acting on MpeA-C83 (17, 18), we hypothesized that the corresponding enzymes in CA4-
137 B strains, MpeW and MpeQ (Fig. 1A), could be a PEB lyase and PEB lyase-isomerase, respectively, both also
138 acting on MpeA. To test this hypothesis, we created *mpeW*⁻ and *mpeQ*⁻ insertion mutants in the CA4-B strain
139 A15-62. Comparison of fluorescence excitation spectra revealed that for GL-grown cultures, Exc_{495:545} was
140 increased in the *mpeW*⁻ mutant compared to the wild-type (WT), whereas no difference was observed under
141 BL (Fig. 3A-B). Conversely, no difference could be seen between Exc_{495:545} of *mpeQ*⁻ mutants and WT under
142 GL, while the Exc_{495:545} ratio dramatically decreased in BL-grown *mpeQ*⁻ mutants compared to WT (Fig. 3C-D).
143 Both mutants still exhibited some levels of chromatic acclimation, since the Exc_{495:545} ratio changed from 1.17
144 ± 0.01 in GL to 1.68 ± 0.07 in BL for *mpeW*⁻ and from 0.74 ± 0.02 in GL to 0.91 ± 0.01 in BL for *mpeQ*⁻, as
145 compared to 0.74 ± 0.01 in GL and 1.72 ± 0.09 in BL for WT cells (all data are average ± SE; n = 2). Based on
146 these results, we hypothesized that i) MpeW is required for PEB attachment, while MpeQ is required for PEB
147 attachment and isomerization to PUB and ii) both are acting on one or possibly two chromophore binding
148 cysteine(s), but seemingly not all three sites that change chromophorylation during the CA4 process. The
149 CA4 phenotype of both mutants could be restored with the re-introduction of WT *mpeW* or *mpeQ* genes in
150 *trans* (Fig. 3 and *SI Appendix*, Fig. S6).

151 Since in the CA4-A strain RS9916, the transcript levels of the lyase-isomerase *mpeZ* were found to be
152 about 32-fold higher in BL than GL (12), while the *mpeY* lyase levels were similar in both colors (18), we also
153 checked the light color response of the counterparts *mpeQ* and *mpeW* genes in the CA4-B strain A15-62.
154 Real-time PCR expression data showed that while *mpeQ* is not significantly differentially regulated between
155 GL and BL, *mpeW* is 44.26 ± 1.34-fold (average ± SD; n=3) more expressed in GL than BL (*SI Appendix*, Fig.
156 S7).

157

158 ***mpeW* and *mpeQ* Mutants Differ from the WT by the Chromophore Attached to MpeA-C83 in Green and**
159 **Blue Light, Respectively.** To identify the biochemical changes responsible for the differences in whole-cell
160 fluorescence, PBS were purified from the *mpeW* and *mpeQ* mutants and PEI and PEII subunits separated by
161 HPLC. Absorption spectra only differed between WT and mutants for MpeA (Fig. 2 and *SI Appendix*, Fig. S2).
162 Indeed, compared to the WT, MpeA from the *mpeW* mutant had a lower PEB absorption peak at 550 nm in
163 GL (Fig. 2A), whereas MpeA from the *mpeQ* mutant exhibited a PEB peak at 550 nm in BL not seen in WT
164 cells (Fig. 2D). This confirmed that both MpeW and MpeQ are involved in MpeA chromophorylation, with
165 MpeW being responsible for PEB attachment and MpeQ for PEB attachment and simultaneous isomerization
166 to PUB. Tandem mass spectrometry of CpeA and MpeA, the two PE subunits that change chromophorylation
167 during CA4 (see above), further showed that the *mpeW* mutant mainly differed from the WT by having a
168 PUB instead of a PEB at MpeA-C83 in GL, whereas the *mpeQ* mutant differed from the WT by having a PEB
169 instead of a PUB at MpeA-C83 in BL (Table 1 and *SI Appendix*, Fig. S8-9). Surprisingly, both WT and mutants
170 displayed a mixed chromophorylation at MpeA-C140 in GL. The slightly higher proportion of PUB in mutants
171 compared to the WT (35% and 15%, respectively; Table 1) could suggest that MpeQ and MpeW might also
172 have a role in the chromophorylation changes occurring during CA4 at this position. If true, this effect is likely
173 indirect, since no chromophorylation of MpeA-C140 could be detected in our recombinant assays (see
174 below).

175

176 **Recombinant MpeW and MpeQ are Both Acting on MpeA-C83.** Activities of MpeW and MpeQ were tested
177 using a heterologous plasmid coexpression system in *Escherichia coli*. Four different hexahistidine-tagged
178 (HT-) versions of recombinant MpeA were used as substrates in the coexpressions: A15-62 and RS9916 HT-
179 MpeA; a mutant RS9916 MpeA with C83 replaced by alanine, RS9916 HT-MpeA(C83A); and a mutant RS9916

180 MpeA with C75 and C140 each replaced with alanine, RS9916 HT-MpeA(C75A, C140A). RS9916 HT-MpeB and
181 RS9916 HT-CpeA were also used to further test the substrate preference. These phycobiliprotein subunits
182 were co-expressed with PEB synthesis enzymes and with either MpeW or MpeQ, purified and their spectral
183 properties analyzed. The negative control (A15-62 HT-MpeA expressed with PEB synthesis enzymes but
184 without any lyase) showed no detectable fluorescence (Fig. 4A, C). The coexpressions of MpeA (either from
185 A15-62 or RS9916) and either MpeW or MpeQ confirmed that the former attached PEB while the latter
186 attached PUB to both versions of MpeA (Fig. 4A-D), while coexpressions of MpeW or MpeQ and either MpeB
187 or CpeA demonstrated that neither had lyase activity on these two proteins. Coexpressions of MpeW and
188 mutants RS9916 MpeA, in which cysteine residues are replaced by alanine [RS9916 MpeA (C83A) or (C75A,
189 C140A)] further showed that PEB was covalently bound to MpeA-C83 (Fig. 4A-B). The same system was used
190 to demonstrate that MpeQ also acted specifically on MpeA-C83 by ligating PEB and isomerizing it to PUB (Fig.
191 4C-D). The minor fluorescence emission peak at ~600 nm in the *mpeW* system (Fig. 4A) is likely coming from
192 PEB that is not held in a stretched conformation.

193 Collectively, these results indicate that in the CA4-B process, MpeW is the lyase responsible for the
194 attachment of PEB to MpeA-C83 in GL while MpeQ is the lyase-isomerase responsible for the attachment of
195 PEB and its isomerization to PUB at MpeA-C83 in BL.

196

197

198 Discussion

199

200 With six phycobilin binding sites per α - β monomer, PEII is the most pigmented phycobiliprotein known so
201 far in the *Cyanobacteria* phylum (7, 19), and the ecological success of marine *Synechococcus* spp. is likely tied

202 with this biological innovation, as evidenced by the large predominance of PEII-containing cells (so-called PT
203 3) in open waters of the world ocean (9). Gain of PEII, which is thought to have occurred by duplication and
204 divergence from the corresponding PEI encoding genes (20), also implied the concomitant acquisition of
205 enzymes necessary for its proper chromophorylation (5). In this context, the diversification of the MpeQWYZ
206 enzyme family, which belongs to the E/F structural clan (16) and likely derived by duplication and divergence
207 from a *cpeY*-like gene ancestor (Fig. 1) (21, 22), has been pivotal for the development of CA4, the only
208 example among the six chromatic acclimation forms known so far in *Cyanobacteria* to involve color-induced
209 changes only in chromophore content (23). The fact that CA4 seemingly appeared twice during the evolution
210 of marine *Synechococcus*, with CA4-A and -B occurring in most cases in phylogenetically distant lineages and
211 colonizing different light niches (Fig. 1) (9, 12) is particularly intriguing. Although the molecular mechanism
212 underpinning CA4-A is starting to be understood (13, 17, 18), CA4-B was thus far biochemically
213 uncharacterized, and the differences between the two CA4 systems remained unclear. Here, we show that
214 CA4-B is mechanistically similar to CA4-A, since it also involves two enzymes that vie for the same binding
215 site on α -PEII subunit (MpeA) and whose gene expressions are differentially regulated by the ambient light
216 color (*SI Appendix*, Fig. S10). We demonstrate that MpeW is a phycobilin lyase attaching PEB at MpeA-C83 in
217 GL, whereas MpeQ is a phycobilin lyase-isomerase binding PUB at the same position in BL. Intriguingly, the
218 CA4-B-specific lyase/lyase-isomerase MpeW/Q pair exhibits a reversed activity compared to its counterpart
219 pair MpeZ/Y in the CA4-A strain RS9916 (*SI Appendix*, Fig. S10). Indeed, the lyase-isomerase *mpeZ* was found
220 to be upregulated under BL, while in the CA4-B process the lyase *mpeW* is upregulated under GL. In both
221 cases, expression of the gene coding for the second enzyme of the couple is not differentially expressed
222 between GL and BL (12, 13, 17). Our data therefore sheds light on a fascinating dual-enzyme co-evolution
223 process that explains the co-occurrence of two mutually exclusive CA4 types in the marine *Synechococcus*
224 radiation. Our data provide strong evidence for the previously proposed hypothesis (23, 24) that the “basal
225 state” for CA4-A strains (i.e., in absence of CA4) corresponds to a GL specialist phenotype (low PUB:PEB ratio)

226 and that CA4 confers these cells the ability to change their spectral properties upon BL illumination, by
227 inducing the expression of the phycobilin lyase-isomerase MpeZ. Conversely, the “basal state” for CA4-B
228 strains would correspond to a BL specialist phenotype (high PUB:PEB ratio), CA4 providing these cells the
229 ability to acclimate to GL by inducing the synthesis of the PEB lyase MpeW. Thus, in both cases, CA4 appears
230 to be a “plug-and-play” mechanism that adds on top of the existing basal chromophorylation. This view is
231 further supported by the gathering into a small dedicated genomic island of genes necessary for CA4,
232 including the regulators *fciA* and *fciB* and one phycobilin lyase (either *mpeZ* or *mpeW*; Fig. 1A). Furthermore,
233 the absence of any allelic difference between PBS genes of PT 3c and 3dB strains (Fig. 1C; see also (9)) might
234 suggest that the CA4-B island is more readily transferred between *Synechococcus* strains through horizontal
235 gene transfer than is the CA4-A island. Surprisingly however, the latter displays several typical genomic island
236 features, including a biased GC content compared to the surrounding genomic context and presence in the
237 vicinity of the island of hotspots for DNA recombination such as tRNA or *psbA* genes, which are absent in the
238 case of the CA4-B island (12, 17). So, the mechanism by which a CA4-B island could be transferred from a PT
239 3dB strain to a BL specialist (PT 3c) and the frequency of such transfers remain unclear.

240 It is also interesting to note that, as previously observed for *mpeZ* and *mpeY^{3dA-}* mutants in the CA4-A
241 strain RS9916 (17, 18), both *mpeW* and *mpeQ* CA4-B mutants still showed some degree of chromatic
242 acclimation, variations of the $Exc_{495:545}$ ratio observed in the *mpeW* and *mpeQ* mutants representing about
243 51% and 18% of that occurring in the WT, respectively (Fig. 2C-D). In both lyase-isomerase mutants (*mpeZ*
244 and *mpeQ*), $Exc_{495:545}$ is strongly decreased in BL (about 0.8) compared to the WT (1.5-1.6), but higher than
245 in GL (0.6-0.7 for both mutants and WT; Fig. 2C-D and (17)). Similarly, both lyase mutants (*mpeY* and *mpeW*)
246 had an increased $Exc_{495:545}$ in GL relative to the WT (about 1.1 vs. 0.6), but still lower than in BL [1.5-1.6 for
247 both; Fig. 2A-B and (18)]. This suggests that other genes are involved in CA4. In the absence of any obvious
248 other CA4-specific phycobilin lyase, an interesting candidate could be the conserved hypothetical gene
249 *unk10*, which is present in both versions of the CA4 genomic island and strongly overexpressed in BL in the

250 CA4-A strain RS9916 (12, 17, 23). Future characterization of this unknown gene as well as the putative
251 regulator *fcic*, present in CA4-A but not CA4-B islands (Fig. 1A and *SI appendix* Fig. S10), will help unravel the
252 different regulatory mechanisms behind this remarkable dual light color acclimation process, which strongly
253 impact the ecology and photophysiology of a key component of marine phytoplankton communities.

254

255

256 **Materials and Methods**

257

258 **Phylogenetic Analyses.** Sequences used in this study (MpeQ, W, Y, Z) can be found in Dataset S1. Briefly,
259 MpeQ, W, Y and Z protein sequences were aligned using MAFFT 7.299b L-INS-I algorithm (25). Pairwise
260 identity between sequences was computed from this alignment using BioPython. Best model for
261 phylogenetic reconstruction corresponded to LG aa substitution model with empirical base frequencies (F),
262 gamma model of rate heterogeneity (G) and invariable sites (I) as selected with ProtTest 3.4.1 (26). Tree
263 search was conducted using RAxML 8.2.9 (27) without the rapid hill-climbing heuristic (-f o). 100 tree
264 searches were conducted starting from randomized maximum parsimony tree (default), and 100 searches
265 starting from fully random trees (-d). Best tree was selected and 250 bootstraps performed. Tree was plotted
266 using ETE3 (28). The same procedure was used to generate a tree with CpeY sequences to root the tree
267 represented in Fig. 1C.

268

269 **Strains and Growth Conditions.** *Synechococcus* strain A15-62 was obtained from the Roscoff Culture
270 Collection (<http://roscoff-culture-collection.org>; RCC strain 2374). It was originally isolated near Cape Verde
271 (Atlantic Ocean) from 30 m depth (29). Both wild-type and mutant strains were routinely grown at 22°C in
272 PCR-S11 (30) in polystyrene flasks (CytoOne, StarLab, USA) at ca. 25 $\mu\text{mol quanta m}^{-2} \text{s}^{-1}$ white light. A15-62

273 mutants were maintained with 50 $\mu\text{g}\cdot\text{mL}^{-1}$ kanamycin. Prior to whole-cell absorption and fluorescence
274 measurements as well as to PBS isolation and separation of phycobiliproteins, WT and mutant strains were
275 acclimated for at least two weeks at 20 $\mu\text{E}\cdot\text{m}^{-2}\cdot\text{s}^{-1}$ BL or GL provided by LED ramps (Luxeon Rebel LED LXML-
276 PB01-0040 and LXML-PM01-0100, respectively; Alpheus, France).

277
278 **Fluorescence measurements.** Spectral properties of WT and mutant strains were measured using a LS-50B
279 spectrofluorimeter (Perkin Elmer, Waltham, MA, USA). Fluorescence excitation was monitored from 420 nm
280 to 560 nm (0.5 nm steps) with emission monitored at 580 nm.

281
282 **Quantitative PCR Analysis of *mpeW* and *mpeQ* Gene Expression.** The expression levels of *mpeQ* and *mpeW*
283 genes was monitored by real time qPCR, as previously described (12). Briefly, triplicate cultures of
284 *Synechococcus* sp. strain A15-62 were acclimated at 20 $\mu\text{mol photons m}^{-2} \text{s}^{-1}$ BL or GL then cells were
285 harvested and RNA extracted. For *mpeW* and the control *rnpB* gene, encoding the RNA component of
286 ribonuclease P, we used previously designed primers (12), while for *mpeQ* gene-specific primers were
287 designed using Primer Blast (National Center for Biotechnology Information, Bethesda, MD; Dataset S3).
288 After optimization steps, reverse transcription and qPCR analyses were performed according to (12). The 2⁻
289 $\Delta\Delta\text{CT}$ method (31) was finally used to quantify the relative fold change in mRNA levels using *rnpB* as a reference
290 gene to normalize the relative transcript levels.

291
292 **Plasmid Construction for *mpeW* and *mpeQ* Disruption and Complementation and Construction of**
293 **Expression Plasmids.** Primers are listed in Dataset S3 and plasmids in Dataset S4. The pMUT100-A15-62-
294 *mpeW* and pMUT100-A15-62-*mpeQ* constructs were made by PCR amplification of an 820-885 bp internal
295 fragment of A15-62 *mpeW* and A15-62 *mpeQ* using the primers pairs Syn_A15-
296 62_*mpeW*_126F_BamHI/999R_SphI and Syn_A15-62_*mpeQ*_123F_EcoRI/983R_SphI (SI Appendix, Fig. S11).

297 The pMUT100 backbone was PCR-amplified using the primer pair pMUT100_1291F_SphI/5535R_BamHI
298 (pMUT100-A15-62-mpeW) or pMUT100_1291F_SphI/5535R_EcoRI (pMUT100-A15-62-mpeQ). Vector and
299 inserts were digested with SphI and either EcoRI or BamHI (NEB) and ligated. Conjugation between *E. coli*
300 MC1061 containing either pMUT100-A15-62-mpeW or pMUT100-A15-62-mpeQ and *Synechococcus* A15-62
301 was performed as previously described (17, 32). Individual colonies were picked and tested for *mpeW* or
302 *mpeQ* disruption by PCR amplification. For complementation, a derivative of the plasmid pRL153
303 (autonomously replicating in marine *Synechococcus*) was first constructed by cloning a lacZ cassette
304 (pBClacZ) into the BamHI/EagI cloning site of pJS1 for convenient screening of *E. coli* colonies (*SI Appendix*,
305 Fig. S11).

306 The pBClacZ-A15-62-mpeW and pBClacZ-A15-62-mpeQ constructs were made by PCR amplification of
307 the promoter and ribosome-binding site of *mpeW* and *mpeQ*, using the primer pairs Syn_A15-
308 62_unk10_38R_BamHI/Syn_A15-62_fciB_892F_EagI and Syn_A15-62_unk9_13R_ApaI/Syn_A15-
309 62_mpeB_56R, respectively (*SI Appendix*, Fig. S11). PCR fragments were digested with EagI and either BamHI
310 (*mpeW*) or ApaI (*mpeQ*) and ligated into similarly digested pBClacZ. Conjugation between *E. coli* MC1061
311 containing either pBClacZ-A15-62-mpeW or pBClacZ-A15-62-mpeQ and *Synechococcus* A15-62 *mpeW* or
312 *mpeQ* was performed as previously described (17, 32). Individual colonies were picked and tested for *mpeW*
313 or *mpeQ* complementation by PCR amplification (*SI Appendix*, Fig. S11).

314
315 **PBS Isolation and separation of phycobiliproteins.** PBS were purified as previously described (33), starting
316 from 10 L of cultures. All steps were performed at room temperature unless specified. Briefly, cells were
317 harvested by centrifugation, washed twice and resuspended in 0.65M phosphate buffer, and lysed twice
318 using a French press system. Membranes and hydrophobic pigments were removed by 1 h incubation with
319 5% w/v Triton X-100 and centrifugation. The red aqueous layer was loaded onto 0.25-1.0M discontinuous
320 sucrose gradient in phosphate buffer, and centrifuged overnight at 22,500 rpm (range: 42,500-91,300 x g) in

321 a SW28 rotor (Beckman Coulter) at 22°C, or 2-3 h at 49,000 rpm (198,000 *g*) in a VTi 50 rotor (Beckman
322 Coulter). Colored bands were collected and frozen at -20°C until analysis (see Fig. 4 in (34) for illustration).

323 Purified PBS were dialyzed in 5 mM sodium phosphate buffer, pH 7.0 with 5mM 2-mercaptoethanol (β -
324 Me) and then concentrated by ultrafiltration using Amicon Ultra-15 centrifugal filters (Millipore; Billerica,
325 MA). A sample containing 500 μ L of a 1:3 ratio of sample to 9 M urea (pH brought to 2.0 with HCl) was
326 prepared prior to HPLC separation. A Waters E2695 pump (Waters Corporation, Milford, MA) was used in
327 conjunction with a Waters 2996 photodiode array and a Thermo-scientific BioBasic-4 HPLC column (Thermo-
328 scientific, Waltham, MA; 250mm x 4.6 mm, 5 μ m particle size) to separate each phycobiliprotein. The
329 program used a flow rate of 1.5 ml min⁻¹ with a gradient program starting at a 65:35 ratio of Buffer A (0.1%
330 trifluoroacetic acid solution with 0.001 M sodium azide) to Buffer B (2:1 acetonitrile:isopropanol in 0.1% TFA
331 with 0.001M sodium azide). The starting conditions are 65% A:35% B. After the sample was injected, after
332 holding for 2 min, buffer conditions were ramped to 100% B over 45 min. The samples were monitored at
333 280 nm, 490 nm, and 550 nm. Separated samples were concentrated using a vacuum centrifuge and stored
334 in the freezer at -20° C until ready for digestion by trypsin.

335
336 **Heterologous expression and purification of recombinant proteins.** For recombinant protein expression,
337 each gene was amplified by PCR from *Synechococcus* RS9916 or A15-62 chromosomal DNA using the primers
338 listed in Dataset S3 and cloned into plasmids as described in Dataset S4. Recombinant proteins were
339 expressed and purified from *E. coli* BL21 (DE3) competent cells (Novagen/EMD Millipore Corp., Darmstadt,
340 Germany) as previously described (35). Once at OD_{600nm}= 0.6, cultures were induced with 1 mM isopropyl 1-
341 thio- β -D-galactopyranoside (IPTG), after which the cells were allowed to grow at 18°C for an additional 24 h
342 before being harvested by centrifugation. HT-proteins were purified as described (36).

343

344 **Protein and bilin analysis by spectroscopy and gel-electrophoresis.** Fluorescence emission and absorbance
345 spectra were acquired on a Perkin Elmer LS55 fluorescence spectrometer (Waltham, MA) and a Lambda 35,
346 dual-beam UV/Vis spectrometer (Perkin Elmer) as previously described (37). Polyacrylamide gel
347 electrophoresis (PAGE, 15% w/v) with sodium dodecyl sulfate (SDS) was used to analyze polypeptide samples
348 acquired after purification of proteins as previously described (17). Zn-enhanced fluorescence of covalently
349 attached bilins was visualized using an imaging system (Bio-Rad MP) with excitation at 460 nm (PUB
350 detection) or 540 nm (PEB detection). Proteins in the gels were then stained by incubation in Coomassie
351 brilliant blue G-250 overnight and de-stained in 10 % methanol and 10 % acetic acid and visualized with trans-
352 white light (Bio-Rad MP).

353

354 **Tryptic digestion and mass spectrometry.** Tryptic digestion of proteins was conducted as previously
355 described (38). Tryptic-digested samples were analyzed using LC-MS/MS on an Orbitrap Lumos Fusion mass
356 spectrometer (Thermo Fisher) with an Agilent 1100 Capillary HPLC as its inlet. LC-MS/MS analysis was
357 performed as previously described with a few modifications (13, 17). Alternatively, some samples were
358 reanalyzed using a Thermo Easy-nLC 1000 capillary LC with the following conditions. Buffer A = 0.1% v/v
359 aqueous formic acid; buffer B = 80% v/v acetonitrile, 0.1% v/v formic acid in water. Load 2 μ l with 0% B onto
360 a 5 mm long, 0.1 mm i.d. C18 trapping column. A 0.075 mm i.d. x 150 mm long C18 analytical column led
361 directly into the nanospray needle. The gradient was 2% B at 0 min, ramp to 7% B at 0.5 min, ramp to 50%
362 B at 20 min, ramp to 100% B at 21 min, hold 100% B for 9 min. The trap column was re-equilibrated 12 μ l of
363 Buffer A and the analytical column with 10 μ l of 2% B between each injection. Mass spectra were recorded
364 continuously at 120,000 resolving power. Data dependent tandem mass spectra were recorded at 30,000
365 resolving power with 3 seconds between MS1 spectra. The tandem mass spectra were processed using
366 Thermo Proteome Discover 2.1 software; a simplified protein database consisting of only the 40 proteins
367 expected to be part of the PBS was used to speed up the analysis. Bilin-containing peptides were confirmed

368 by manual inspection of their associated MS1, MS2, and UV-VIS spectra. Extracted ion chromatograms (EICs)
369 for each of the bilin-containing peptides were generated using XCalibur 4.0 software (Thermo Fisher). Briefly
370 intensities for a 20-ppm window around the masses indicated were extracted and the resulting
371 chromatograms smoothed with a 5-point boxcar algorithm. Areas were computed using the default Genesis
372 algorithm in XCalibur; a combination of UV-VIS spectra confirmation, retention time and tandem MS/MS
373 data were used to differentiate between the PUB and PEB isomers. The ionizability of PEB and PUB modified
374 versions of the same peptide were considered to be identical for comparisons. The areas of multiple peaks
375 corresponding to the same bilin isomer were added together (oxidized versions of PEB-containing peptides
376 sometimes split into more than one peak with nearly identical tandem mass spectra). The PUB fraction was
377 computed by summing the area of all PUB-containing features for a single modified cysteine and dividing it
378 by the total of both PUB and PEB modified versions of features containing the same cysteine.

379

380 **ACKNOWLEDGEMENTS.** This research was supported by the French national agency for research (ANR)
381 programs CINNAMON (ANR-17-CE2-0014) and EFFICACY (ANR-19-CE02-0019) as well as the EU program
382 Assemble+ for F.P and L.G, by National Science Foundation grants to W.M.S. (MCB-1244339 and MCB-
383 2017171) and to D.M.K. (MCB-1818187 and MCB-2017171) and by a Fulbright Fellowship to T.G. This work
384 was also supported by EMBRC-France, managed by the ANR in the "Investments for the Future" program
385 under the reference ANR-10-INSB-02. We also acknowledge the Ecology and Environment Institute (INEE) of
386 the French National Center for Research (CNRS) for facilitating exchanges between the different partner
387 laboratories through the international project of scientific collaboration (PICS) program ChromaCya (2016-
388 19). The Orbitrap Fusion Lumos was purchased with funds from the Indiana University Precision Health
389 Initiative. The Genomer platform (Biogenouest) is warmly thanked for help with sequencing.

390

391 **References**

- 392 1. P. Flombaum, *et al.*, Present and future global distributions of the marine Cyanobacteria
393 *Prochlorococcus* and *Synechococcus*. *Proc. Natl Acad. Sci. U.S.A* **110**, 9824–9829 (2013).
- 394 2. L. Guidi, *et al.*, Plankton networks driving carbon export in the oligotrophic ocean. *Nature* **532**, 465–
395 470 (2016).
- 396 3. M. L. Paulsen, *et al.*, *Synechococcus* in the Atlantic Gateway to the Arctic Ocean. *Front. Mar. Sci.* **3**,
397 191 (2016).
- 398 4. K. Zwirgmaier, *et al.*, Global phylogeography of marine *Synechococcus* and *Prochlorococcus* reveals a
399 distinct partitioning of lineages among oceanic biomes. *Environ. Microbiol.* **10**, 147–161 (2008).
- 400 5. C. Six, *et al.*, Diversity and evolution of phycobilisomes in marine *Synechococcus* spp.: a comparative
401 genomics study. *Genome Biol* **8**, R259 (2007).
- 402 6. W. A. Sidler, “Phycobilisome and phycobiliprotein structure” in *The Molecular Biology of*
403 *Cyanobacteria*, D. A. Bryant, Ed. (Kluwer Academic Publishers, 1994), pp. 139–216.
- 404 7. L. J. Ong, A. N. Glazer, Phycoerythrins of marine unicellular cyanobacteria: I. Bilin types and locations
405 and energy transfer pathways in *Synechococcus* spp. phycoerythrins. *J. Biol. Chem.* **266**, 9515–9527
406 (1991).
- 407 8. L. J. Ong, A. N. Glazer, J. B. Waterbury, An unusual phycoerythrin from a marine cyanobacterium.
408 *Science* **224**, 80–3 (1984).
- 409 9. T. Grébert, *et al.*, Light color acclimation is a key process in the global ocean distribution of
410 *Synechococcus* cyanobacteria. *Proc. Natl. Acad. Sci.* **115**, E2010–E2019 (2018).

- 411 10. B. Palenik, Chromatic adaptation in marine *Synechococcus* strains. *Appl. Environ. Microbiol.* **67**, 991–
412 994 (2001).
- 413 11. C. Everroad, *et al.*, Biochemical bases of type IV chromatic adaptation in marine *Synechococcus* spp. *J*
414 *Bacteriol* **188**, 3345–3356 (2006).
- 415 12. F. Humily, *et al.*, A gene island with two possible configurations is involved in chromatic acclimation
416 in marine *Synechococcus*. *PLoS One* **8**, e84459 (2013).
- 417 13. J. E. Sanfilippo, *et al.*, Self-regulating genomic island encoding tandem regulators confers chromatic
418 acclimation to marine *Synechococcus*. *Proc. Natl. Acad. Sci.* **113**, 6077–6082 (2016).
- 419 14. A. N. Glazer, Light guides. Directional energy transfer in a photosynthetic antenna. *J. Biol. Chem.* **264**,
420 1–4 (1989).
- 421 15. N. Blot, *et al.*, Phycourobilin in trichromatic phycocyanin from oceanic cyanobacteria is formed post-
422 translationally by a phycoerythrobilin lyase-isomerase. *J. Biol. Chem.* **284**, 9290–9298 (2009).
- 423 16. A. Bretaudeau, *et al.*, CyanoLyase: a database of phycobilin lyase sequences, motifs and functions.
424 *Nucleic Acids Res* **41**, D396-401 (2012).
- 425 17. A. Shukla, *et al.*, Phycoerythrin-specific bilin lyase-isomerase controls blue-green chromatic
426 acclimation in marine *Synechococcus*. *Proc. Natl. Acad. Sci.* **109**, 20136–20141 (2012).
- 427 18. J. E. Sanfilippo, *et al.*, Interplay between differentially expressed enzymes contributes to light color
428 acclimation in marine *Synechococcus*. *Proc. Natl. Acad. Sci.* **116**, 6457–6462 (2019).
- 429 19. S. M. Wilbanks, A. N. Glazer, Rod structure of a phycoerythrin II-containing phycobilisome. I.
430 Organization and sequence of the gene cluster encoding the major phycobiliprotein rod components
431 in the genome of marine *Synechococcus* sp. WH8020. *J Biol Chem* **268**, 1226–1235 (1993).

- 432 20. R. C. Everroad, A. M. Wood, Phycoerythrin evolution and diversification of spectral phenotype in
433 marine *Synechococcus* and related picocyanobacteria. *Mol. Phylogenet. Evol.* **64**, 381–392 (2012).
- 434 21. L. A. Carrigee, *et al.*, CpeY is a phycoerythrobilin lyase for cysteine 82 of the phycoerythrin I α -subunit
435 in marine *Synechococcus*. *Biochim. Biophys. Acta - Bioenerg.* **1861**, 148215 (2020).
- 436 22. A. Biswas, *et al.*, Biosynthesis of cyanobacterial phycobiliproteins in *Escherichia coli*:
437 Chromophorylation efficiency and specificity of all bilin lyases from *Synechococcus* sp. strain PCC
438 7002. *Appl. Environ. Microbiol.* **76**, 2729–2739 (2010).
- 439 23. J. E. Sanfilippo, L. Garczarek, F. Partensky, D. M. Kehoe, Chromatic acclimation in cyanobacteria: A
440 diverse and widespread process for optimizing photosynthesis. *Annu. Rev. Microbiol.* **73**, 407–433
441 (2019).
- 442 24. T. Grébert, “Pigment diversity in marine *Synechococcus* sp.: molecular basis, evolution and ecological
443 role,” Université Pierre et Marie Curie - Paris VI, Paris, France. (2017) [https://tel.archives-](https://tel.archives-ouvertes.fr/tel-02422222)
444 [ouvertes.fr/tel-02422222](https://tel.archives-ouvertes.fr/tel-02422222).
- 445 25. K. Katoh, D. M. Standley, MAFFT multiple sequence alignment software version 7: Improvements in
446 performance and usability. *Mol. Biol. Evol.* (2013) <https://doi.org/10.1093/molbev/mst010>.
- 447 26. D. Darriba, G. L. Taboada, R. Doallo, D. Posada, ProtTest 3: Fast selection of best-fit models of protein
448 evolution. *Bioinformatics* (2011) <https://doi.org/10.1093/bioinformatics/btr088>.
- 449 27. A. Stamatakis, RAxML version 8: A tool for phylogenetic analysis and post-analysis of large
450 phylogenies. *Bioinformatics* (2014) <https://doi.org/10.1093/bioinformatics/btu033>.
- 451 28. J. Huerta-Cepas, F. Serra, P. Bork, ETE 3: Reconstruction, analysis, and visualization of phylogenomic
452 data. *Mol. Biol. Evol.* **33**, 1635–1638 (2016).

- 453 29. S. Mazard, M. Ostrowski, F. Partensky, D. J. Scanlan, Multi-locus sequence analysis, taxonomic
454 resolution and biogeography of marine *Synechococcus*. *Environ. Microbiol.* **14**, 372–386 (2012).
- 455 30. R. Rippka, *et al.*, *Prochlorococcus marinus* Chisholm et al. 1992 subsp. *pastoris* subsp. nov. strain PCC
456 9511, the first axenic chlorophyll a_2/b_2 -containing cyanobacterium (Oxyphotobacteria). *Int. J. Syst.*
457 *Evol. Microbiol.* **50**, 1833–1847 (2000).
- 458 31. Schmittgen DT, Livak KJ, Analyzing real-time PCR data by the comparative CT method. *Nat. Protoc.*
459 (2008).
- 460 32. B. Brahamsha, A genetic manipulation system for oceanic cyanobacteria of the genus *Synechococcus*.
461 *Appl. Environ. Microbiol.* **62**, 1747–1751 (1996).
- 462 33. C. Six, L. Joubin, F. Partensky, J. Holtzendorff, L. Garczarek, UV-induced phycobilisome dismantling in
463 the marine picocyanobacterium *Synechococcus* sp. WH8102. *Photosynth. Res.* **92**, 75–96 (2007).
- 464 34. R. M. Mahmoud, *et al.*, Adaptation to blue light in marine *Synechococcus* requires MpeU, an enzyme
465 with similarity to phycoerythrobilin lyase isomerases. *Front. Microbiol.* **8**, 243 (2017).
- 466 35. A. Biswas, *et al.*, Characterization of the activities of the CpeY, CpeZ, and CpeS bilin lyases in
467 phycoerythrin biosynthesis in *Fremyella diplosiphon* strain UTEX 481. *J. Biol. Chem.* **286**, 35509–35521
468 (2011).
- 469 36. N. A. Saunée, S. R. Williams, D. A. Bryant, W. M. Schluchter, Biogenesis of phycobiliproteins: II. CpcS-
470 I and CpcU comprise the heterodimeric bilin lyase that attaches phycocyanobilin to Cys-82 of beta-
471 phycocyanin and Cys-81 of allophycocyanin subunits in *Synechococcus* sp. PCC 7002. *J Biol Chem* **283**,
472 7513–7522 (2008).
- 473 37. C. M. Kronfel, *et al.*, Structural and biochemical characterization of the bilin lyase CpcS from

- 474 *Thermosynechococcus elongatus*. *Biochemistry* **52**, 8663–8676 (2013).
- 475 38. D. M. Arciero, D. A. Bryant, A. N. Glazer, In vitro attachment of bilins to apophycocyanin I: specific
476 covalent adduct formation at cysteinyl residues involved in phycocyanobilin binding in C-phycocyanin.
477 *J. Biol. Chem.* **263**, 18343–18349 (1988).
- 478
- 479

480

Legends to Figures

481 **Fig. 1. Phylogeny and similarity of the different members of the MpeQWYZ phycobilin lyase enzyme family**
 482 **and genomic organization of the corresponding genes.** (A) Comparison of the genomic regions involved in
 483 CA4-A and -B processes. The CA4-A genomic island and the PEII sub-region of the PBS genomic region are
 484 located at two different loci on the chromosome of *Synechococcus* strain RS9916 (top), whereas in strain
 485 A15-62 the CA4-B genomic island is located in the middle of the PBS genomic region, immediately
 486 downstream the phycoerythrin-II (PEII) sub-region (bottom). The two genes characterized in the present
 487 study (*mpeW* and *mpeQ*) are shown as underlined black bold letters, their functional homologs in the CA4-A
 488 strain RS9916 (*mpeY* and *mpeZ*) in black bold letters, and other genes in grey. (B) Mean pairwise percentage
 489 of identity between the protein sequences of MpeW, MpeQ, MpeZ, and MpeY^{3a} and MpeY^{3dA} (encoded by
 490 the two *mpeY* alleles), calculated based on full-length alignments. (C) Maximum likelihood phylogeny
 491 (protein sequences, LG+I+G+F model) of the MpeQWYZ enzyme family. CpeY sequences were used as
 492 outgroup to root the tree. Nodes with bootstrap support >70% and >90% are indicated by empty and filled
 493 black dots, respectively. Sequences of A15-62 used in this study are highlighted in bold black letters, other
 494 sequences discussed in the text are shown in black, while all other sequences in grey.

495

496 **Fig. 2. Absorbance spectra of HPLC-purified phycoerythrin II α -subunit (MpeA) for wild-type (WT)**
 497 ***Synechococcus* sp. A15-62, *mpeW* inactivation mutant (*mpeW*) and *mpeQ* inactivation mutant (*mpeQ*)**
 498 **grown under green light (GL) or blue light (BL).** (A and C) WT or mutant cells grown in GL. (B and D) WT or
 499 mutant cells grown in BL. See *SI Appendix*, Fig. S2 for absorbance spectra of the other phycoerythrin-I and II
 500 subunits.

501 **Fig. 3. Whole-cell fluorescence excitation spectra for wild-type (WT) *Synechococcus* sp. A15-62 and mutant**
502 **strains.** WT, *mpeW*⁻ mutant and *mpeW*⁻ complemented strains grown either in GL (A) or BL (B). WT, *mpeQ*⁻
503 and *mpeQ*⁻ complemented strains grown either in GL (C) or BL (D). Fluorescence emission spectra are
504 normalized at 545 nm. Emission was set at 580 nm. Measurements shown here were repeated twice
505 (biological replicates). See *SI Appendix*, Fig. S6 for complementation control.

506

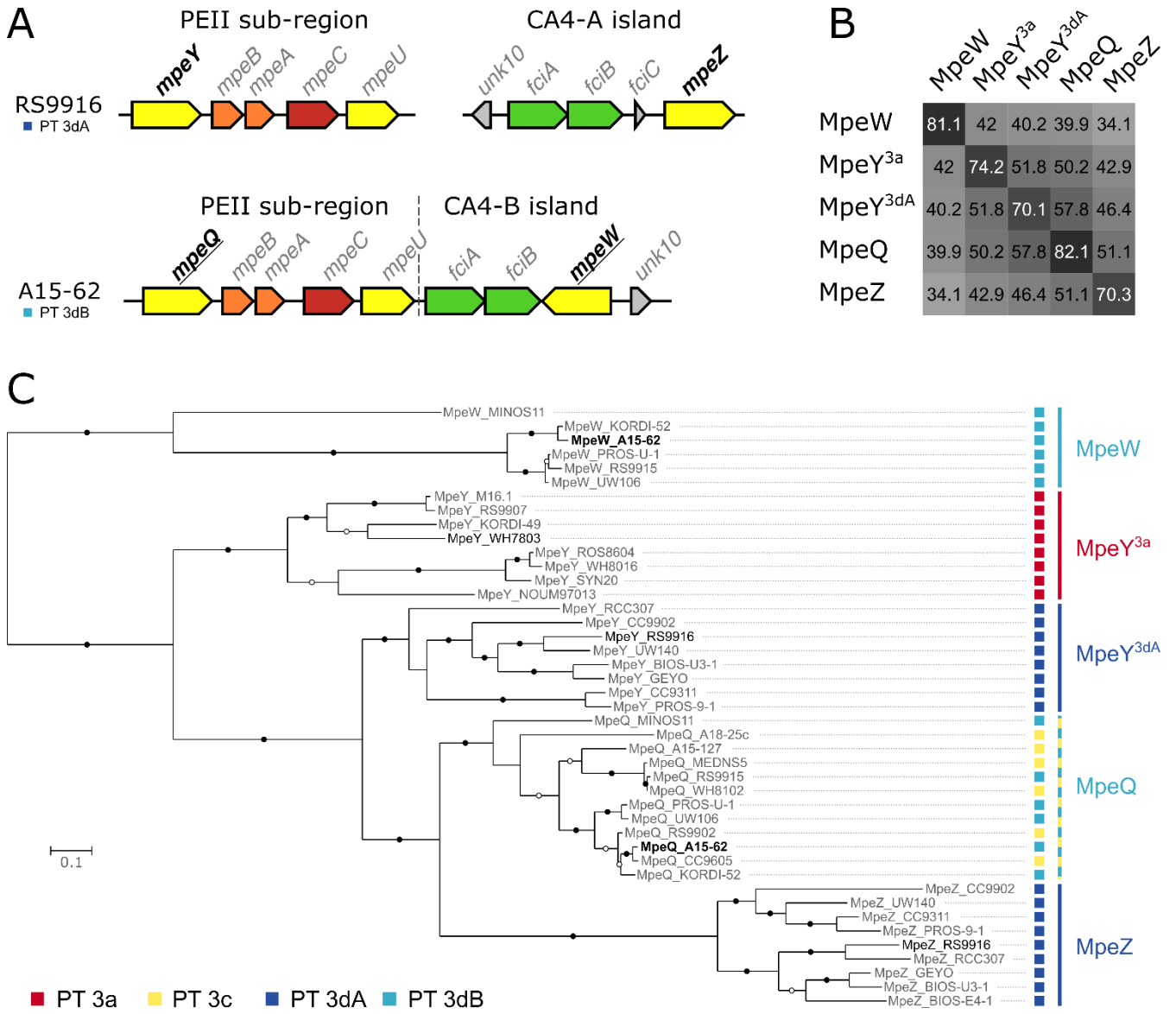
507 **Fig. 4. Determination of the phycobiliprotein subunit and binding site specificities of the MpeW and MpeQ**
508 **enzymes.** Recombinant phycoerythrin-II (PEII) α -subunit (MpeA) from *Synechococcus* sp. A15-62, PElI α - and
509 β -subunits (MpeA, MpeB) and PEI α -subunit (CpeA) from RS9916 as well as site-mutated RS9916 MpeA in
510 which either Cys-83 only or both Cys-75 and Cys-140 were replaced by an alanine [so-called MpeA (C83A)
511 and MpeA (C75A, C140A), respectively], were co-expressed with either MpeQ (A, B) or MpeW (C, D) from
512 A15-62 along with genes necessary for PEB synthesis. (A and C) Absorbance (solid lines) and fluorescence
513 emission (dotted lines) spectra of PEB (panel A, excitation set at 490 nm) or PUB (panel C, excitation set at
514 440 nm) of purified recombinant WT and site-mutated MpeA from RS9916. The secondary emission peak at
515 610 nm in panel A likely corresponds to PEB at C83 (see text). (B and D) Zinc-enhanced fluorescence of SDS-
516 PAGE gel showing relative PEB or PUB covalently bound to different recombinant phycoerythrin subunits
517 under various coexpression conditions (indicated on top) for MpeW (B) or MpeQ (D). Data shown here are
518 representative of three technical replicates.

519

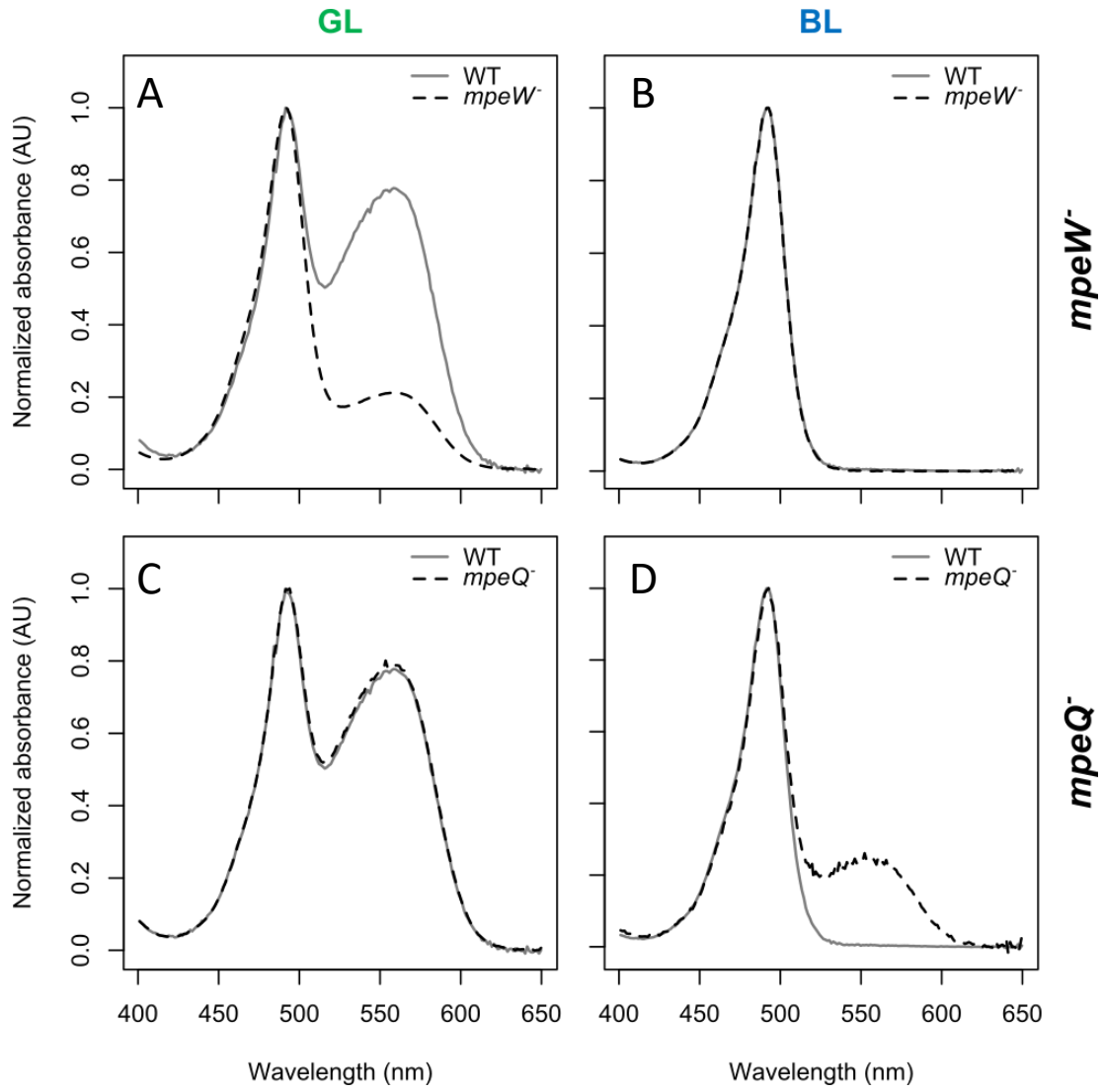
520 **Table 1: Percentage of PUB chromophores, expressed as a PUB/(PEB+PUB) ratio, found at the different**
 521 **cysteinylyl sites of the PEI and PEII α - (CpeA, MpeA) and β -subunits (CpeB, MpeB) in *Synechococcus* sp. A15-**
 522 **62 wild type cells and *mpeW* and *mpeQ* mutants grown under GL and BL.** Underline indicate that the
 523 chromophorylation was confirmed by LC-MS/MS mass spectrometry. Bold indicate that the chromophore is
 524 expected to change during the CA4 process. At some sites, the mass spectrometry analysis detected a mix of
 525 PUB and PEB and the percentage of PUB (%PUB) is indicated. Abbreviations: BL, blue light; GL green light;
 526 ND, not determined; PBP, phycobiliprotein; PEB, phycoerythrobilin; PEI, phycoerythrin I; PEII, phycoerythrin
 527 II; PUB, phycourobilin; WT, wild-type.

PBP	Subunit	Cysteine position	%PUB attached in GL			%PUB attached in BL		
			WT	<i>mpeW</i>	<i>mpeQ</i>	WT	<i>mpeW</i>	<i>mpeQ</i>
PEII	MpeA	75	<u>100</u>	<u>100</u>	<u>100</u>	<u>100</u>	<u>100</u>	<u>100</u>
		83	<u>9</u>	<u>99</u>	<u>2</u>	<u>100</u>	<u>99</u>	<u>14</u>
		140	<u>15</u>	<u>35</u>	<u>36</u>	<u>93</u>	<u>99</u>	<u>99</u>
PEII	MpeB	50,61	100	ND	ND	100	ND	ND
		82	<u>0</u>	ND	ND	<u>0</u>	ND	ND
		165	<u>0</u>	ND	ND	<u>0</u>	ND	ND
PEI	CpeA	82	<u>0</u>	<u>0</u>	<u>0</u>	<u>0</u>	<u>0</u>	<u>0</u>
		139	<u>0</u>	<u>100</u>	<u>21</u>	<u>100</u>	<u>98</u>	<u>43</u>
PEI	CpeB	50,61	100	ND	ND	100	ND	ND
		82	<u>0</u>	ND	ND	<u>0</u>	ND	ND
		159	<u>0</u>	ND	ND	<u>0</u>	ND	ND

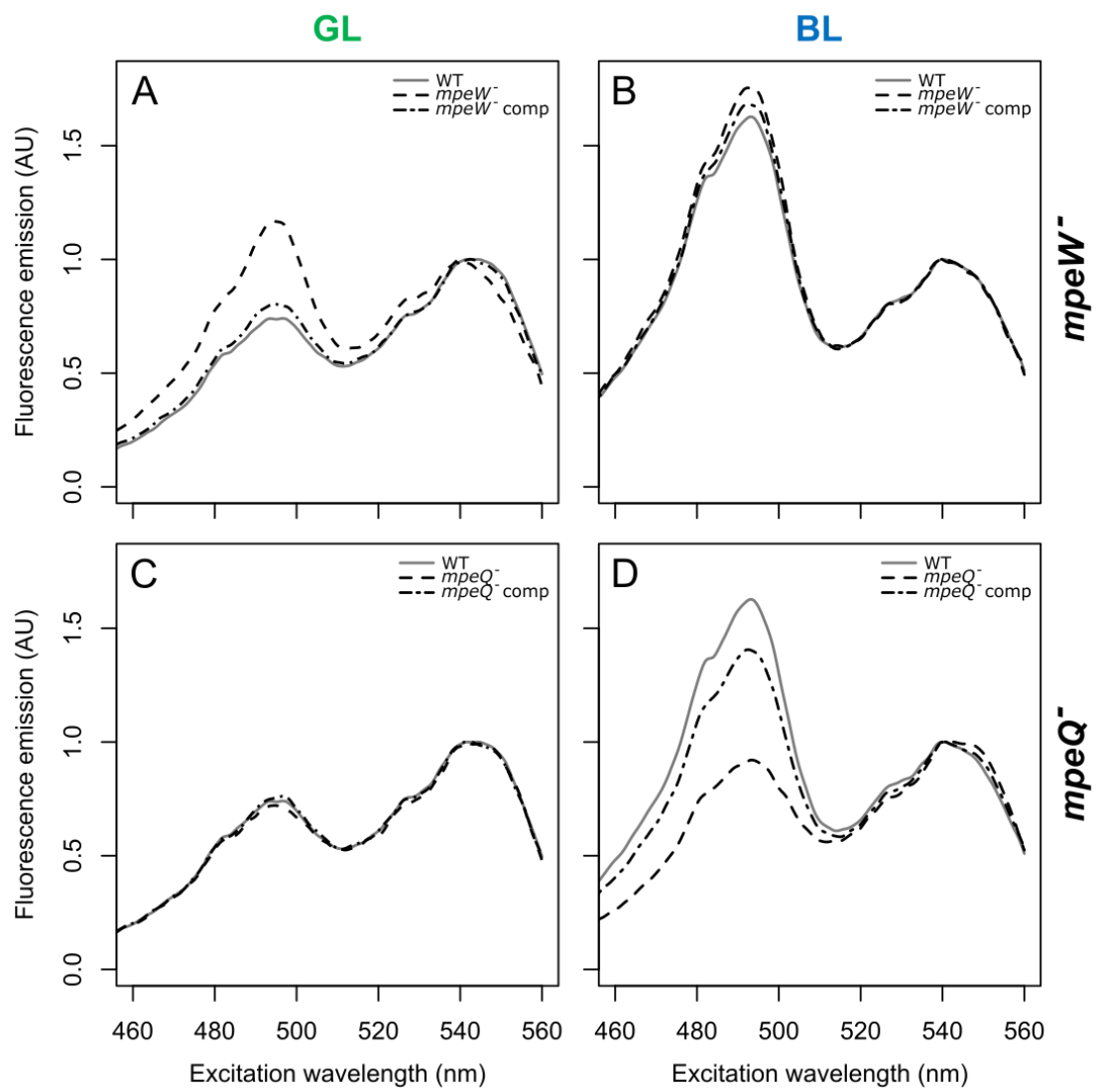
528



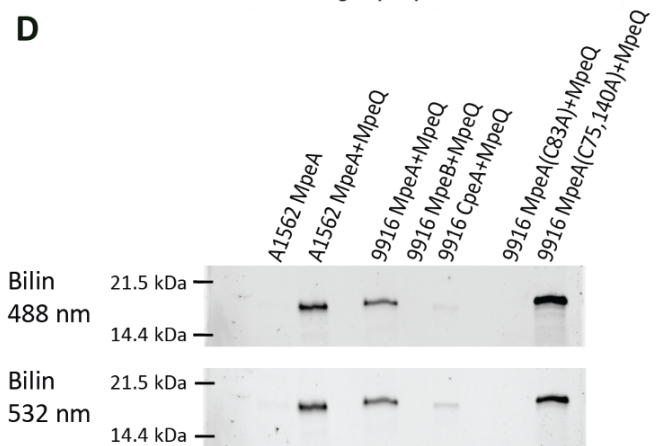
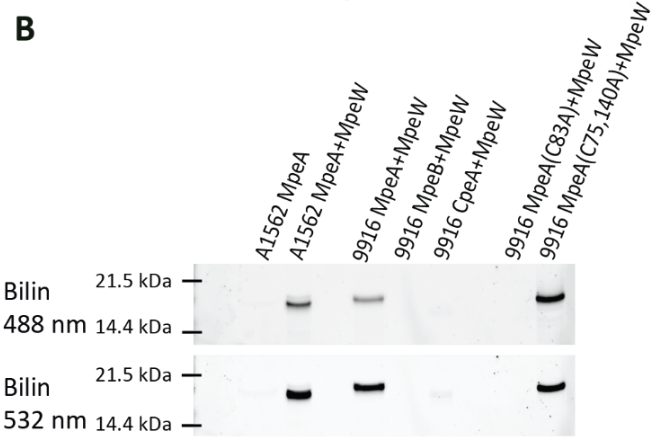
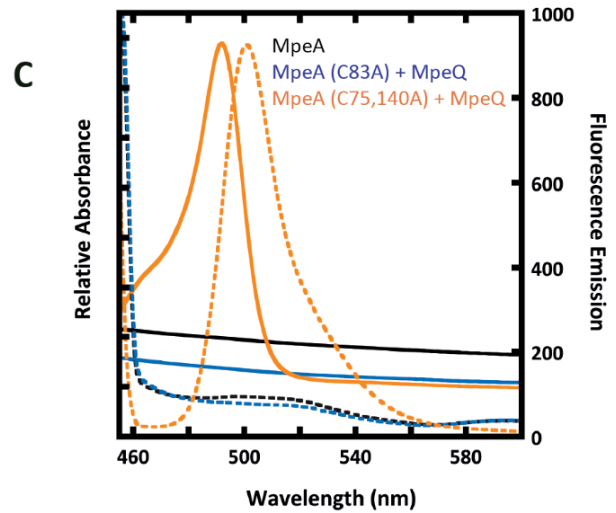
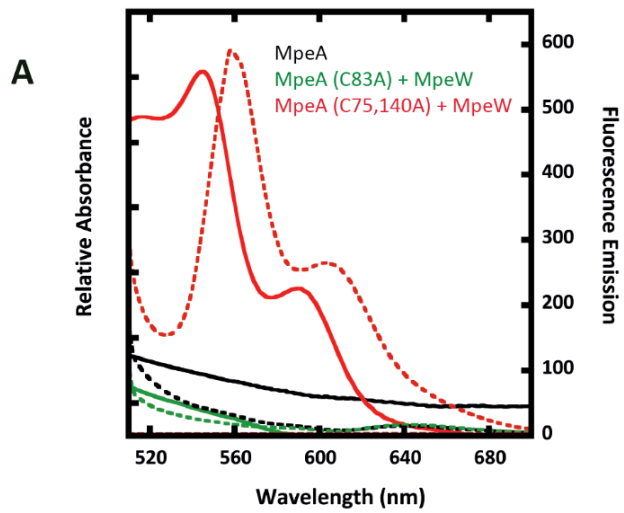
Grébert *et al.*, Figure 1



Grébert *et al.*, Figure 2



Grébert *et al.*, Figure 3



Grébert *et al.*, Figure 4

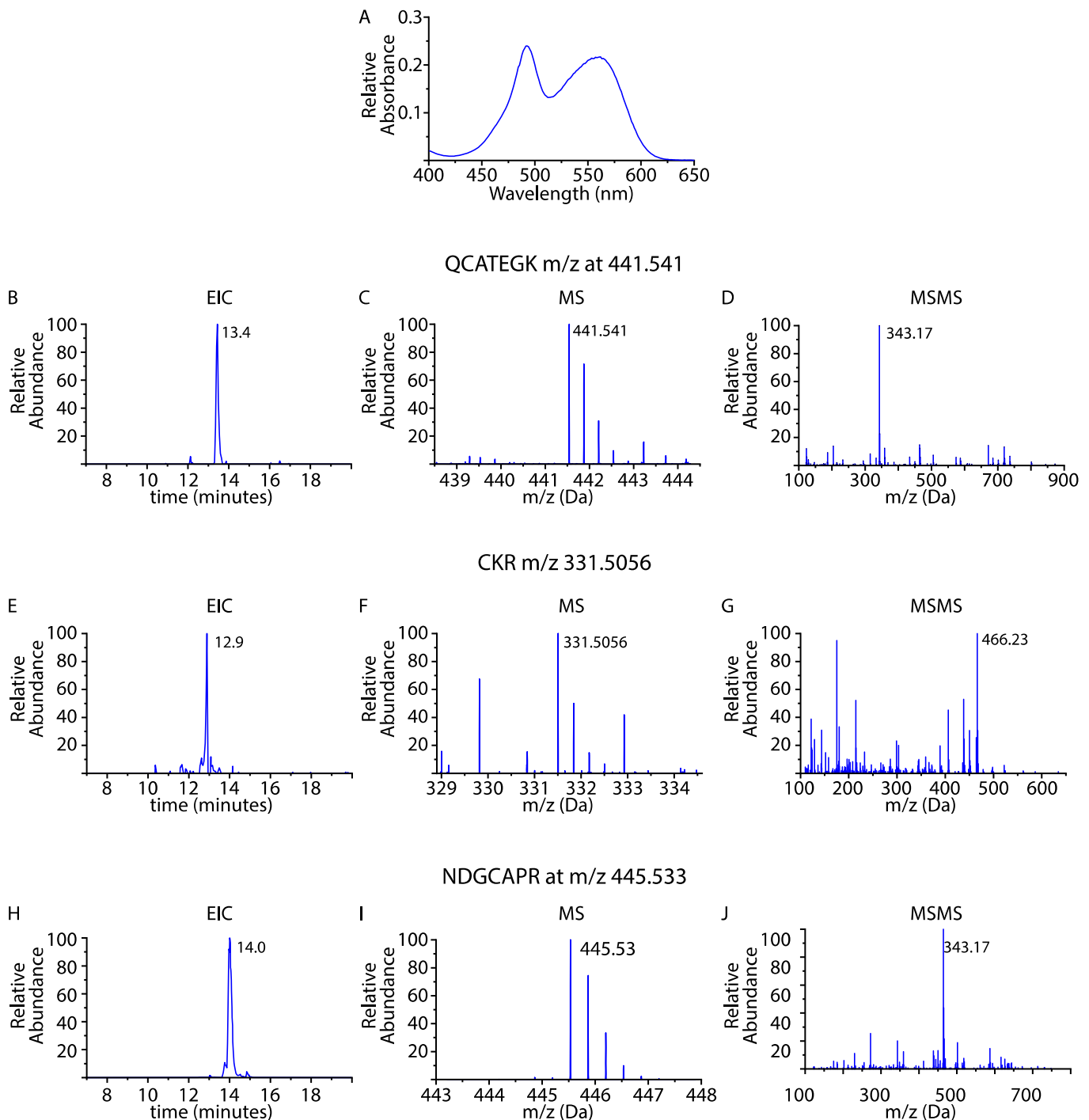


Fig. S1. Absorption spectrum and mass spectrometry analysis of bilin chromophorylation of *Synechococcus* sp. WH7803 phycoerythrin-II α -subunit (MpeA). (A) UV-VIS spectrum from the purified *Synechococcus* WH7803 MpeA showing absorbance peaks at 490 and 550 nm, indicating that the protein is binding both PUB and PEB. (B) LC-MS analysis showing the EIC at mass 441.541 for the bilin-modified peptide QC*₇₅ATEGK showing an elution peak at 13.4 min. (C) MS scan of the elution at 13.4 min showing the isotope profile of a peptide with m/z 441.541. (D) Tandem mass spectrum of m/z 441.5410 at 13.4 min. The relatively early elution and strong diagnostic ion at m/z 343.17 indicate that it binds with PUB. (E) LC-MS analysis showing the EIC at mass 331.506 for the bilin-modified peptide C*₈₃KR showing primarily a single species eluting at 12.9 min. (F) The MS scan confirms the expected mass at 331.506. (G) The strong relative abundance of the diagnostic ion at m/z 466.23, demonstrated the presence of PEB. (H) LC-MS analysis showing the EIC at mass 445.533 for the bilin-modified peptide NDGC*₁₄₀APR showing an elution peak at 14.0 min. (I) MS scan of the elution at 14.0 min showing the isotope profile of a peptide with m/z 445.533. (J) Database interpretation of the MS/MS fragmentation spectra from the 445.533 peptide confirmed the sequence as NDGC*₁₄₀APR. The relatively early elution and strong diagnostic ion at m/z 343.17 indicate modification with PUB. Abbreviations: EIC, extracted ion chromatograph; LC, liquid chromatography; MS, mass spectrometry; PEB, phycoerythrobin; PUB, phycourobilin.

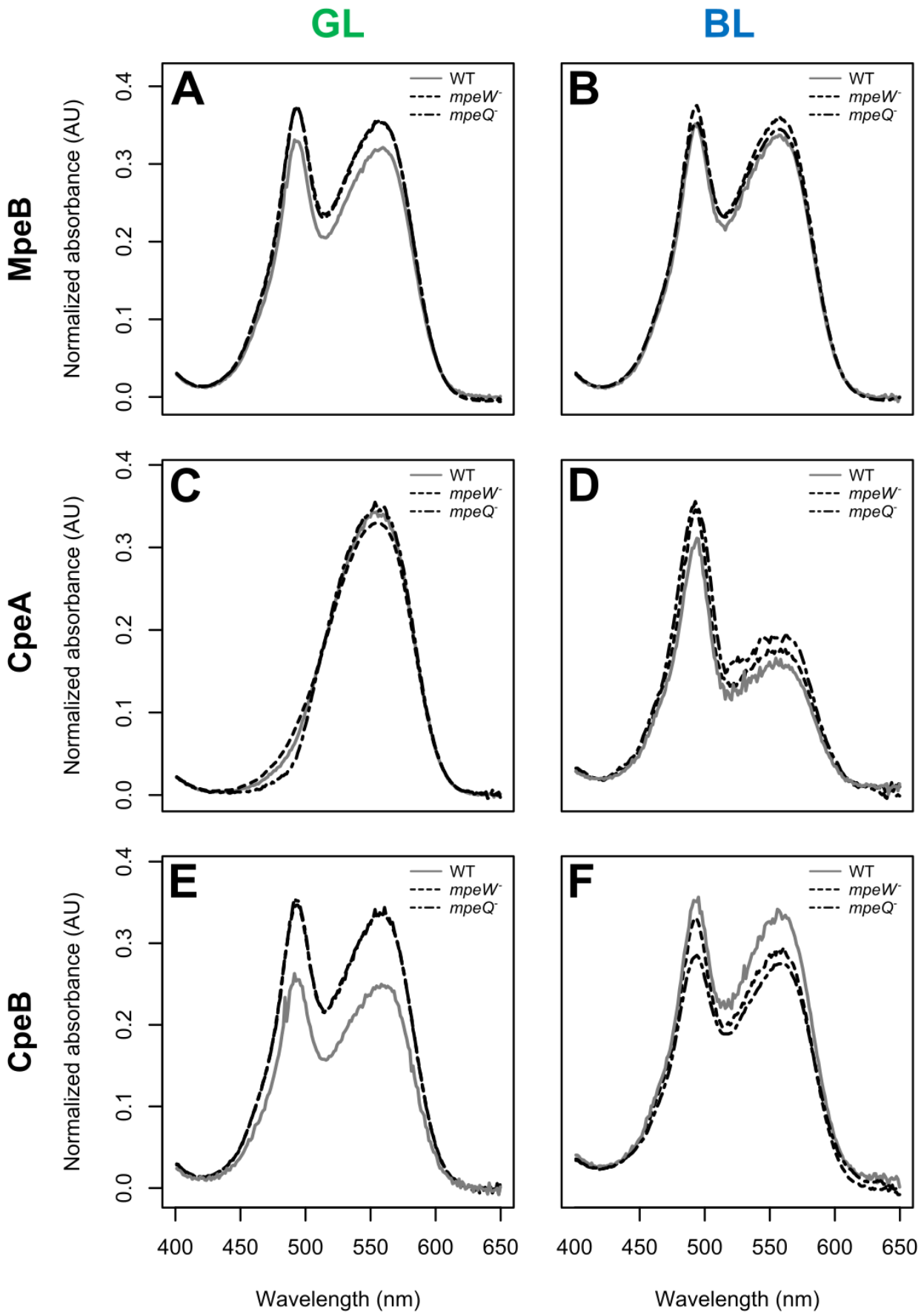


Fig. S2. Absorbance spectra of HPLC-purified phycoerythrin-II β -subunit (MpeB), phycoerythrin-I α - (CpeA) and β - (CpeB) subunits of *Synechococcus* sp. A15-62 WT, *mpeW* inactivation mutant (*mpeW*⁻) and *mpeQ* inactivation mutant (*mpeQ*⁻) cells grown under GL or BL. (A, C and E) WT or mutant grown in GL. (B, D and F) WT or mutant grown in BL. (A and B) MpeB. (C and D) CpeA. (E and F) CpeB. See Fig. 2 for absorbance spectra of MpeA. Abbreviations: BL, blue light; GL, green light.

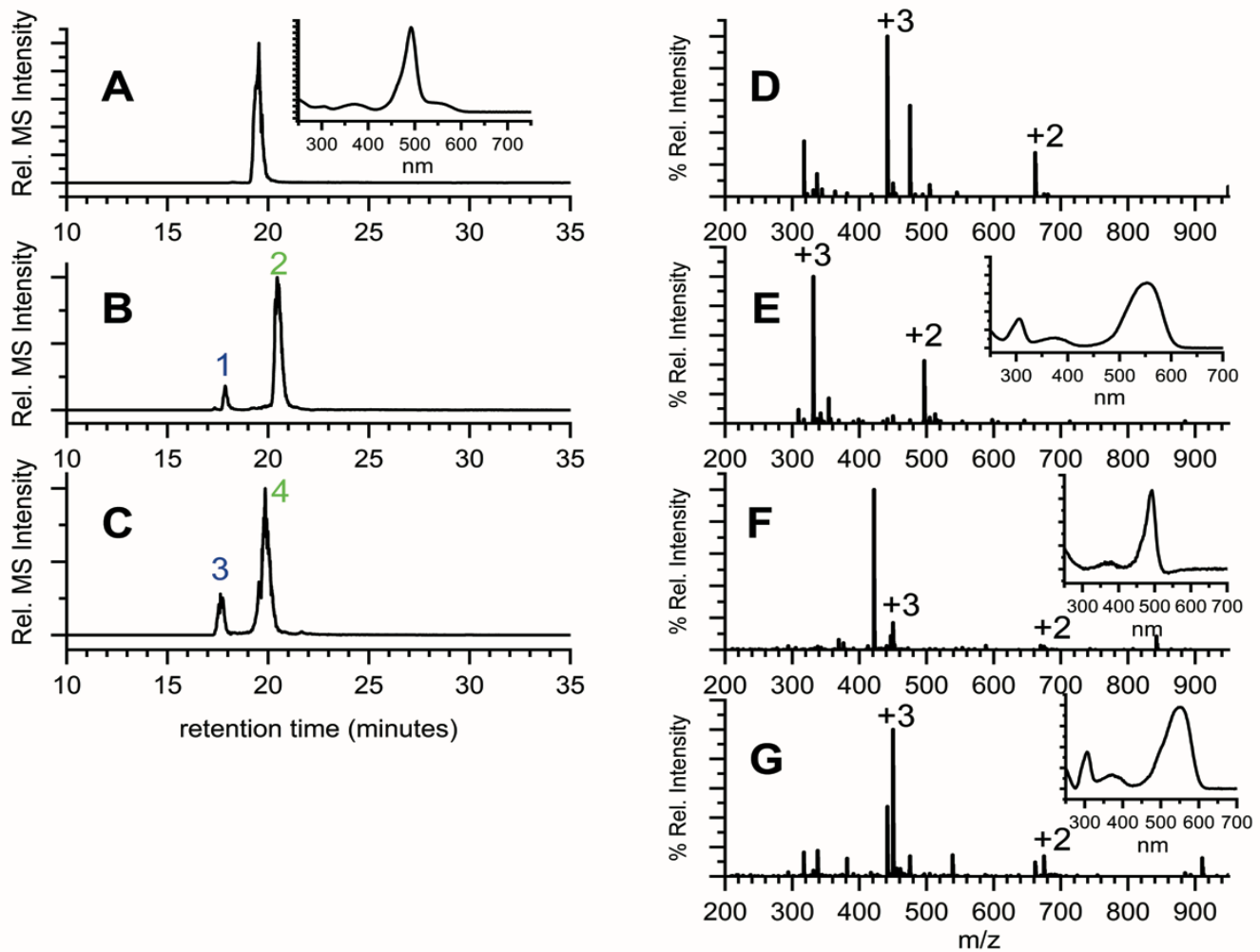


Fig. S3. Mass spectrometry analysis of phycoerythrin-II α -subunit (MpeA) isolated from *Synechococcus* sp. A15-62 wild-type cells grown in GL. (A) EIC for m/z 441.5532, $KC^*_{75}ATEGK^{3+}$ where the * corresponds to a Cys modified by PUB. (B) EIC for m/z 336.8372, $C^*_{83}KR^{3+}$, where the * corresponds to Cys modified by PUB (peak 1) or PEB and oxidation (peak 2). (C) EIC for m/z 450.2204, $SRGC^*_{140}APR$, where the * corresponds to Cys modified by PUB (peak 3) or PEB and oxidation (peak 4). (D) MS data for the 19.5 min peak in panel A. (E) MS data for peak 2 in panel B; inset UV-VIS spectrum at 19.5 min indicates PEB on Cys_{140} . (F) MS from 17.60 min peak 3 in C; UV-VIS spectrum indicates PUB modified Cys. (G) MS data for the 19.9 min peak 4 in panel C; UV-VIS indicates PEB modified Cys. The charge states refer to (peptide+nH) $^{n+}$ ions. Abbreviations: EIC, extracted ion chromatograph; GL, green light; MS, mass spectrometry.

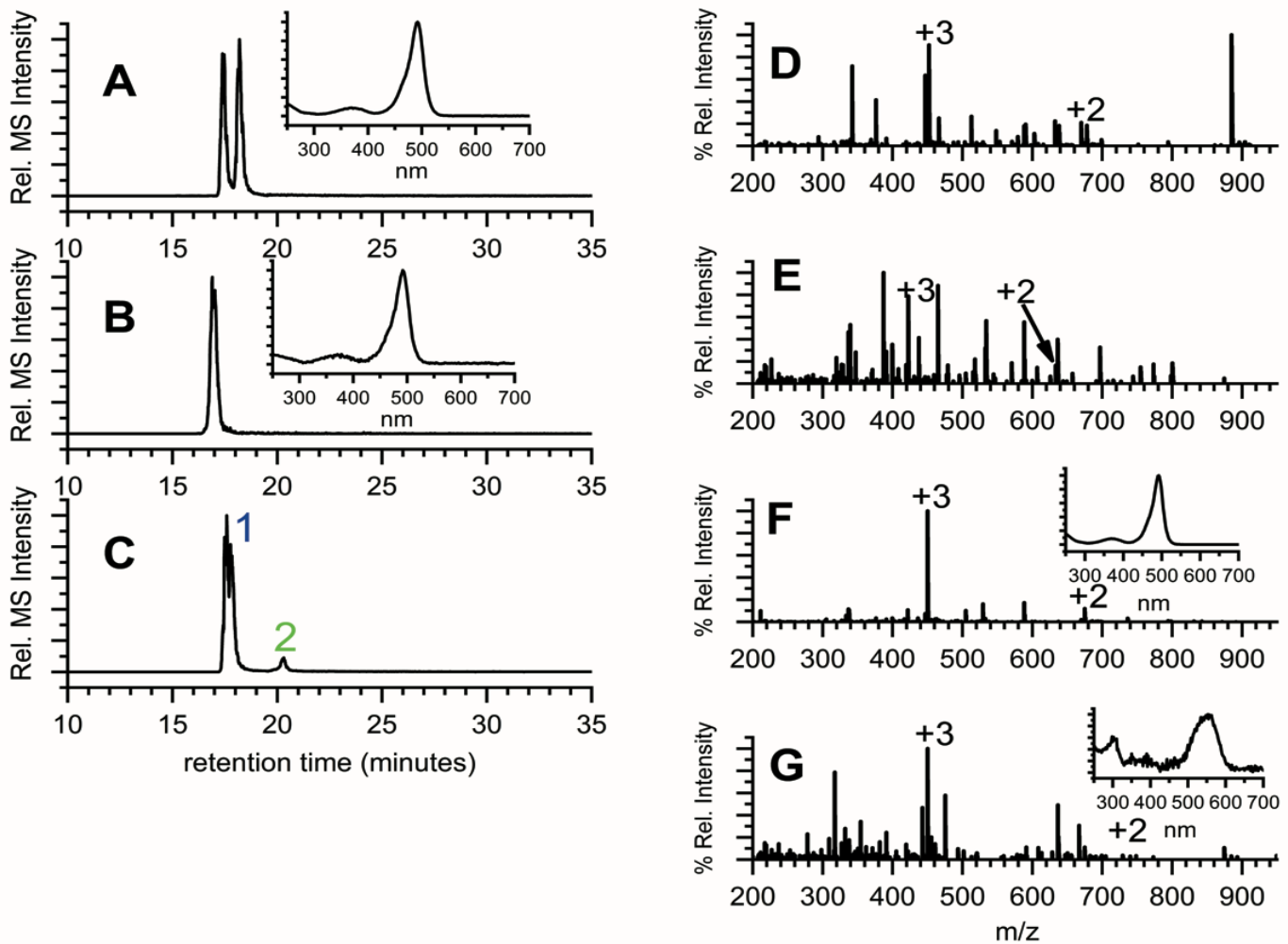
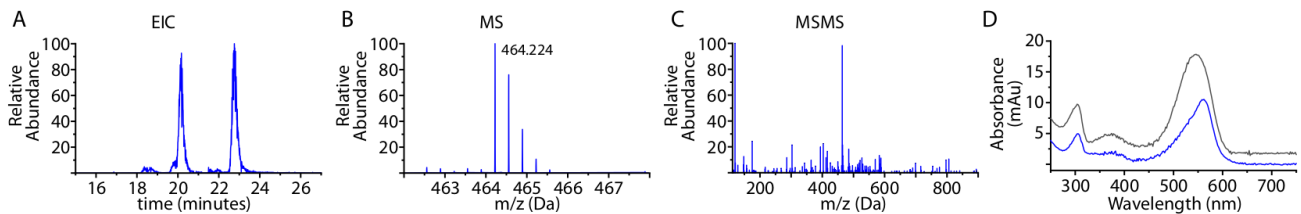
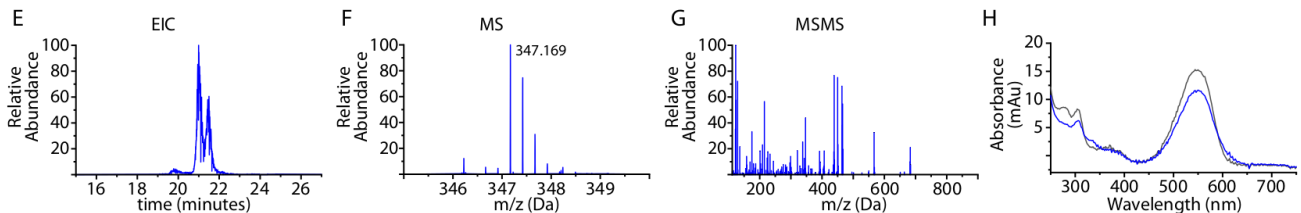


Fig. S4. Mass spectrometry data for phycoerythrin-II α -subunit (MpeA) isolated from *Synechococcus* sp. A15-62 wild-type cells grown in BL. (A) EIC for m/z 446.8848, $KC^*_{75}ATEGK^{3+}$, where the * corresponds to Cys modified by PUB and oxidation. (B) EIC for m/z 422.5498, $EKC^*_{83}KR^{3+}$. (C) EIC for m/z 450.2204, $SRGC^*_{140}APR$. (D) MS data for the 18.20 min peak in panel A (17.39 min peak in panel A gave similar MS, MS-MS, and UV-VIS spectra). (E) MS data for the 16.90 min peak in panel B. (F) MS data for the 17.60 min peak in panel C (peak 1); UV-VIS spectrum indicates PUB modified Cys. (G) MS data for the 20.31 min peak in panel C (peak 2); UV-VIS indicates PEB modified Cys. The charge states indicated in the MS refer to (peptide+nH) $^{n+}$ ions. Abbreviations: BL, blue light; MS, mass spectrometry; EIC, extracted ion chromatograph.

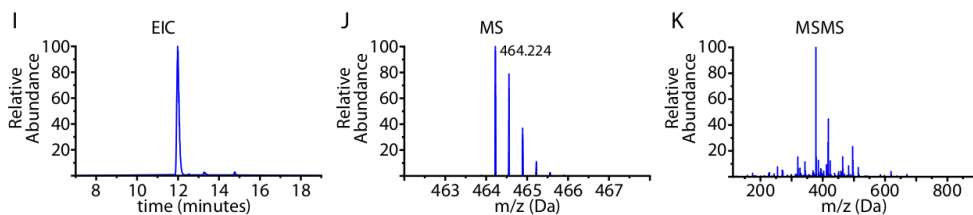
DRACAPR Green Light m/z at 464.224



VDKCYR Green Light m/z at 347.169



DRACAPR Blue Light m/z at 464.224



VDKCYR Blue Light m/z at 462.557

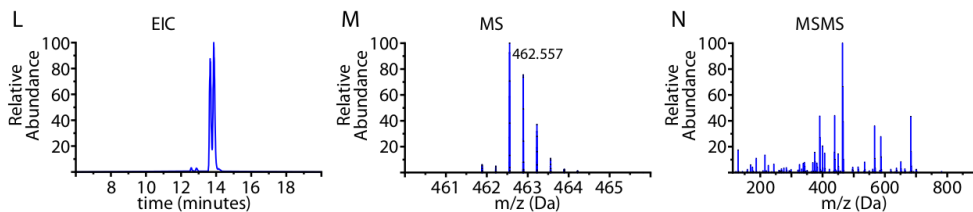


Fig. S5. Tandem mass spectrometry data for phycoerythrin- α -subunit CpeA-C82 and C139 isolated from for A15-62 WT cells grown in GL and BL. (A) LC-MS profile showing the EIC at mass 464.224 for the oxidized version of the bilin-modified peptide DRAC*₁₃₉APR grown in GL with a doublet eluting at 20.1 and 22.8 min. (B) MS scan of the elution at 20.1 min showing the isotope profile of a peptide with the expected m/z of 464.224. (C) Database interpretation of the MS-MS fragmentation spectra from this 464.224 peptide confirmed the sequence as DRAC*₁₃₉APR. (D) UV absorbance spectra at 20.1 min (black) and 22.8 min (blue), with absorbance maxima at 550 nm, indicating both species are modified with PEB. (E) LC-MS profile showing the EIC at mass 347.169 for the oxidized version of the bilin-modified peptide VDKC*₈₂YR grown in GL with a doublet eluting at 20.1 and 21.1 min. (F) MS scan of the elution averaged from 20.9 to 21.2 min showing the isotope profile of a peptide with the expected m/z of 347.169. (G) Database interpretation of the MS/MS fragmentation spectra from this 347.2 peptide confirmed the sequence as VDKC*₈₂YR. (H) UV absorbance spectra at 20.1 min (black) and 21.1 min (blue), with absorbance maxima at 550 nm, indicating that both species are modified with PEB. (I) LC-MS profile showing the EIC at mass 464.224 for the oxidized version of the bilin-modified peptide DRAC*₁₃₉APR grown in blue light eluting at 11.88 min. (J) MS scan of the elution at 11.88 min showing the isotope profile of a peptide with the expected m/z of 464.224. (K) Database interpretation of the MS/MS fragmentation spectra from this 464.224 peptide confirmed the sequence as DRAC*₁₃₉APR. (L) LC MS showing the EIC at mass 462.557 for the bilin-modified peptide VDKC*₈₂YR grown in BL with a peak eluting in a doublet at 13.65 and 14.17 min. (M) MS scan of the elution at 13.65 min showing the isotope profile of a peptide with the expected m/z of 462.557. (N) Database interpretation of the MS/MS fragmentation spectra from this 462.557 peptide confirmed the sequence as VDKC*₈₂YR. This sample was run without UV/VIS collection, but retention time and tandem MS-MS data from other samples with UV/VIS data were used to differentiate between the PUB and PEB isomers of these peptides. Abbreviations: BL, blue light; EIC, extracted ion chromatogram; GL, green light; LC, liquid chromatography; MS, mass spectrometry; PEB, phycoerythrobilin; PUB, phycourobilin.

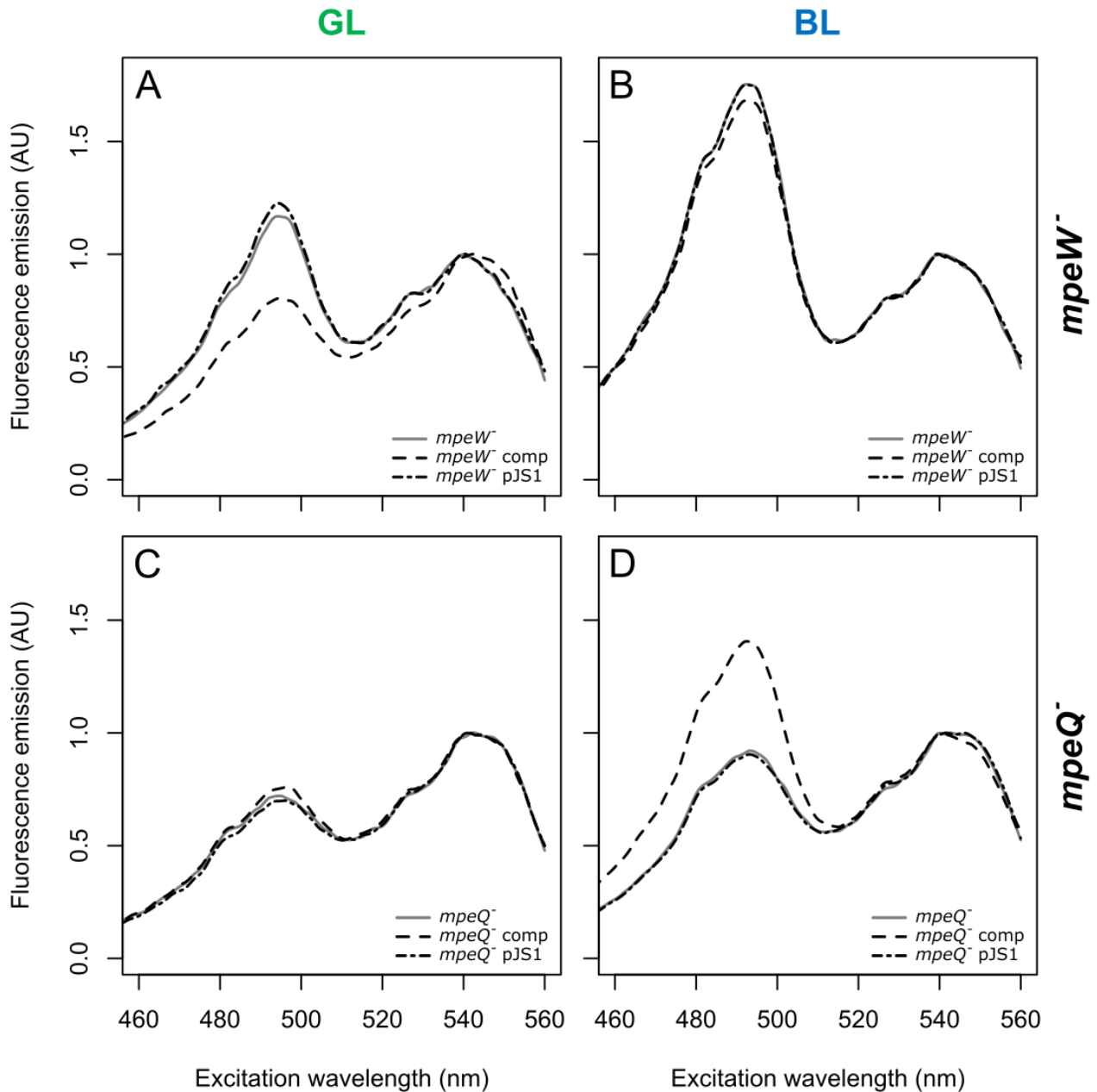


Fig. S6. Whole-cell fluorescence excitation spectra for *Synechococcus* sp. A15-62 mutant and complemented strains. The *mpeW* inactivation mutant (*mpeW*⁻), *mpeQ* inactivation mutant (*mpeQ*⁻), complementation strains *mpeW*⁻ comp (*mpeW*⁻ mutant with plasmid pTG_A15-62_ *mpeW*_comp) and *mpeQ*⁻ comp (*mpeQ*⁻ mutant with plasmid pTG_A15-62_ *mpeQ*_comp) as well as complementation controls *mpeW*⁻ pJS1 and *mpeQ*⁻ pJS1 (*mpeW*⁻ and *mpeQ*⁻ mutants with empty plasmid pJS1) were acclimated for at least two weeks in either green light (GL) or blue light (BL) before the measurement. (A, B) *mpeW*⁻ mutant, complemented and complementation control strains. (C, D) *mpeQ*⁻ mutant, complemented and complementation control strains. Fluorescence emission spectra are normalized at 545 nm for panels A and B and at 495 nm for panels C and D. Emission was set at 580 nm. Measurements were repeated twice (biological replicates).

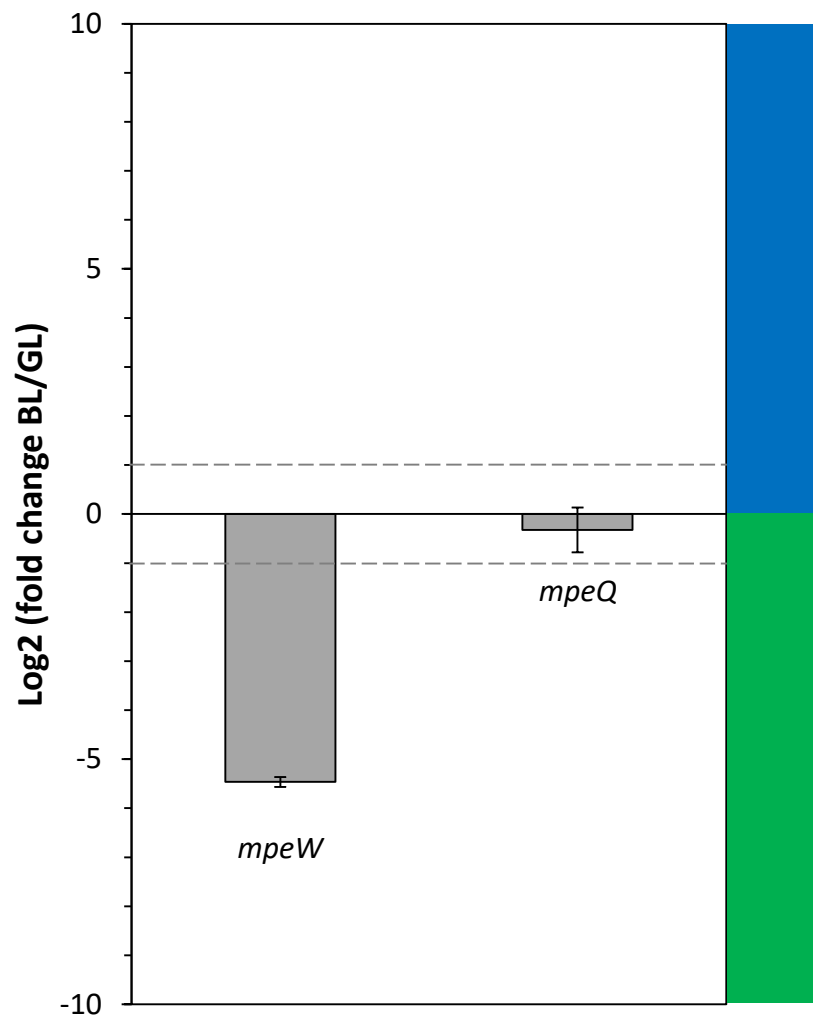


Fig. S7. Differential expression of *mpeW* or *mpeQ* genes in WT *Synechococcus* sp. A15-62 cultures acclimated to 20 $\mu\text{mol photons m}^{-2} \text{s}^{-1}$ blue and green light, as measured by real time PCR. Mean and standard deviation were calculated from three biological replicates. Only differential transcript levels above or below the dotted lines ($\log_2(\text{FC}) > 1$ or < -1) are significant.

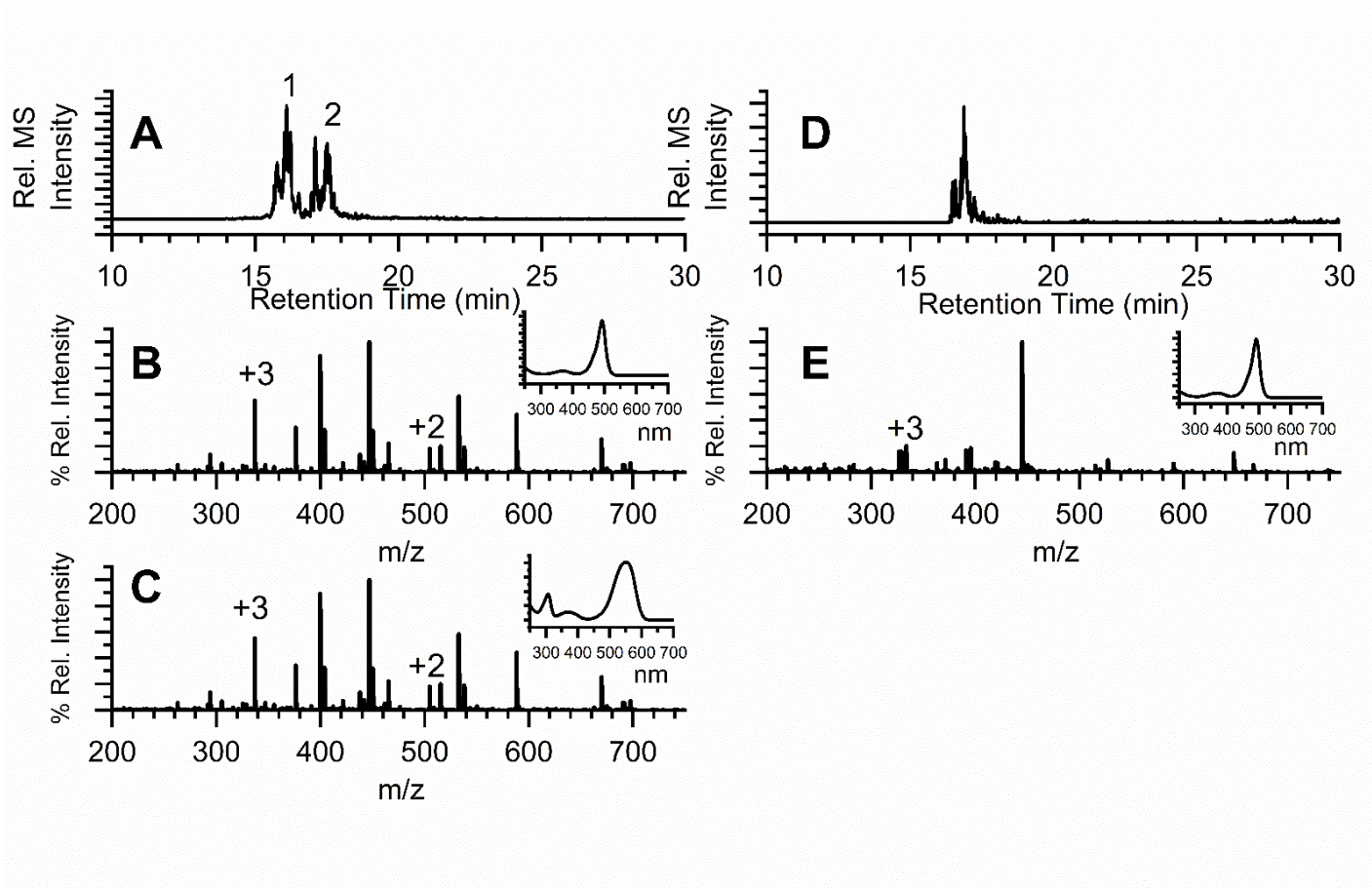


Fig. S8. Mass spectrometry analyses of the phycoerythrin-II α -subunit MpeA-C83 peptides isolated from *Synechococcus* sp. A15-62 *mpeQ*⁻ mutant cells grown in GL and BL. (A) EIC for C*₈₃KR+bilin+oxygen (m/z 336.8372³⁺) in GL. (D) EIC for C*₈₃KR+bilin (m/z 331.5056³⁺) in BL. (B) Mass spectra and UV-VIS spectra (insert) for the 16.1 min peak (peak 1 in panel A). (C) Mass spectra and UV-VIS spectra (insert) for the 17.5 min peak (peak 2 in panel A). (E) Mass spectra and UV-VIS spectra (insert) for the 16.9 min peak in panel (D). Charges labeled in mass spectra indicate peaks arising from C*₈₃KR peptides. Abbreviations: BL, blue light; EIC, Extracted ion chromatograms; GL, green light.

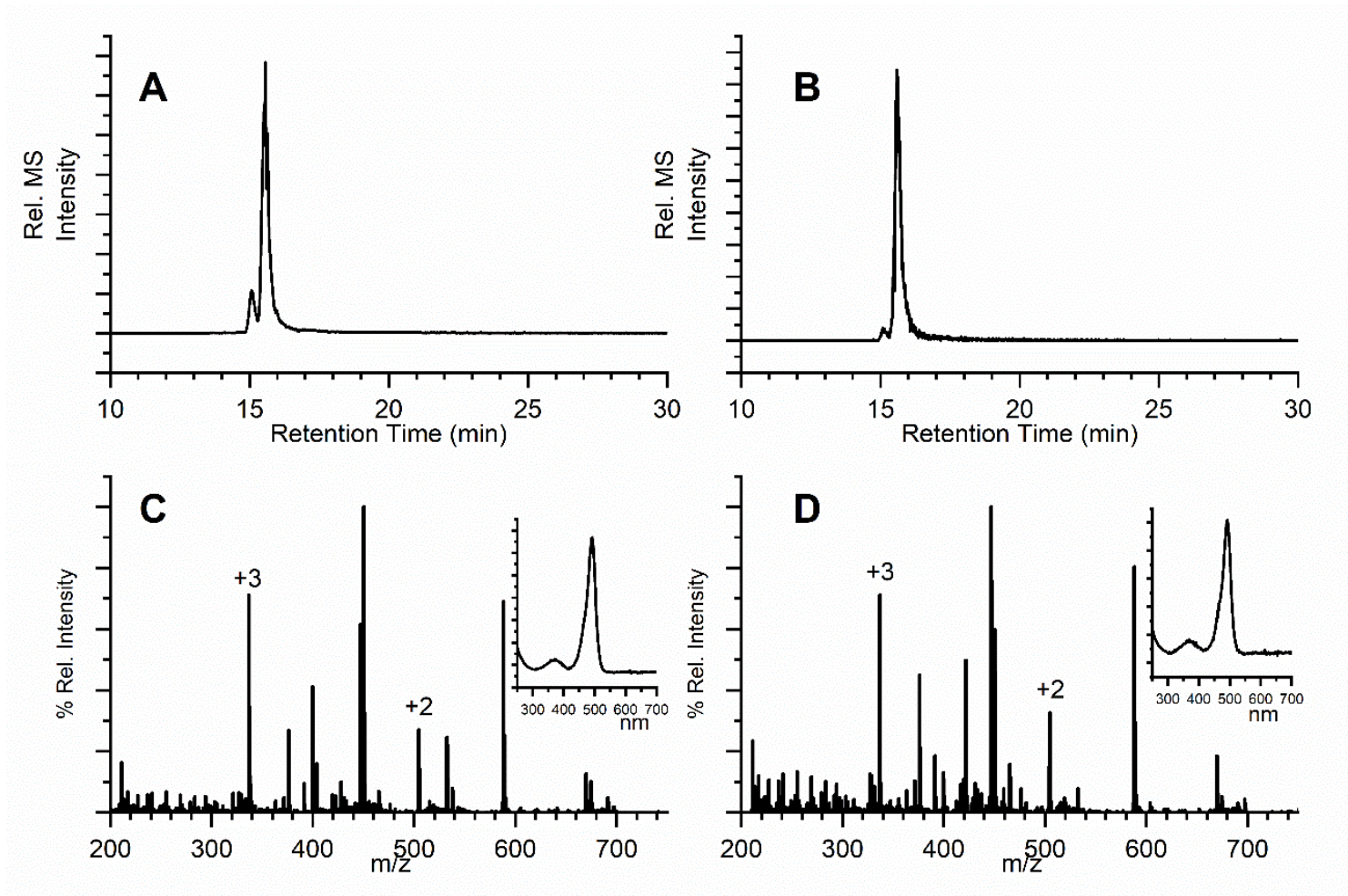


Fig. S9. Mass spectrometry analyses of the phycoerythrin-II α -subunit MpeA-C83 peptides isolated from *Synechococcus* A15-62 *mpeW* mutant cells grown in GL and BL. EIC for C*₈₃KR+ bilin+oxygen (m/z 336.8373³⁺) grown in (A) BL and (B) GL. (C-D) Mass spectra and UV-VIS spectra (insert) from 15.6 min peak in panels A and B, respectively. Both peptides were shown to contain PUB. BL, blue light; EIC, Extracted ion chromatograms; GL, green light.

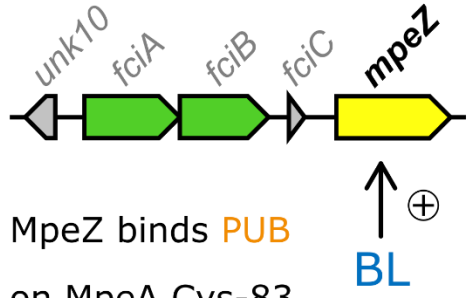
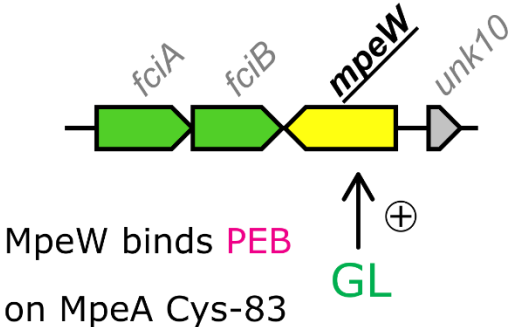
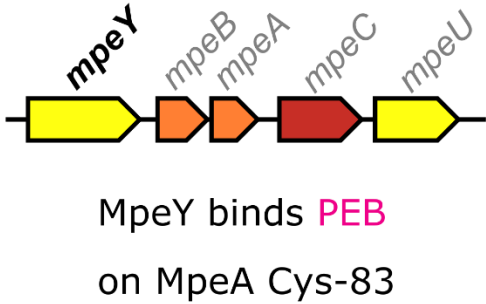
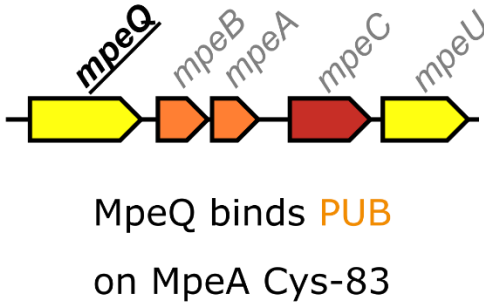
Model strain	RS9916	A15-62
Clade	IX	IIc
Pigment type	3dA	3dB
CA4 island	<p>CA4-A</p>  <p>MpeZ binds PUB on MpeA Cys-83</p>	<p>CA4-B</p>  <p>MpeW binds PEB on MpeA Cys-83</p>
PBS region	 <p>MpeY binds PEB on MpeA Cys-83</p>	 <p>MpeQ binds PUB on MpeA Cys-83</p>
References	(1, 2)	This study

Fig. S10. Summary of the differences between the two types of chromatic acclimation (CA4-A and –B) occurring in marine *Synechococcus*. The table summarizes the main characteristics of the model strains and recapitulates the results from two previous studies on CA4-A using RS9916 and how they compare to the new results obtained in the present study on CA4-B using A15-62. The ‘PBS region’ refers to the genomic region that gathers most genes involved in the biosynthesis and regulation of phycobilisome rods (3). Phylogenetically, both strains belong to sub-cluster 5.1 but to different (sub)clades *sensu* (4).

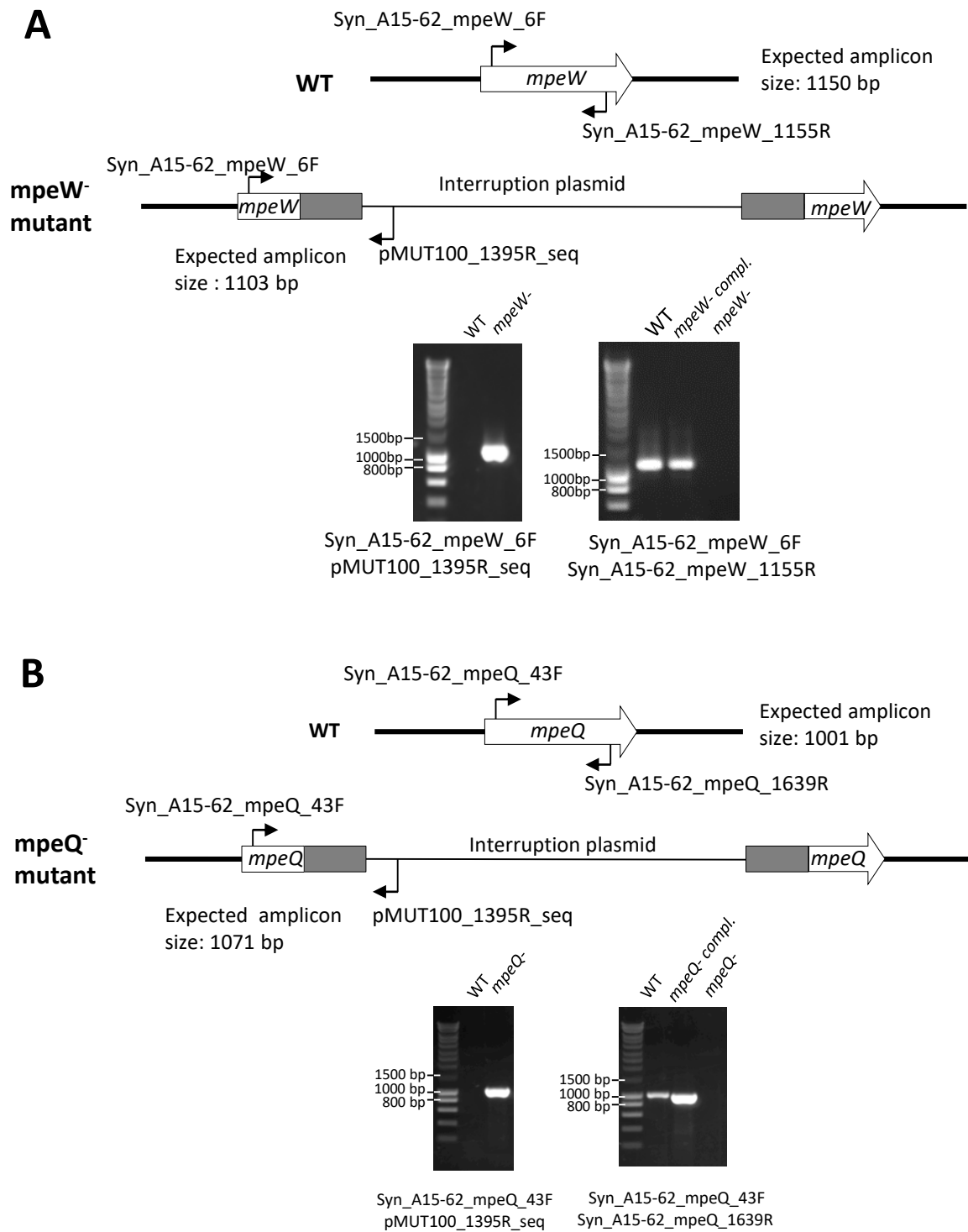


Fig. S11. Constructions of *mpeW/Q* mutants and complementations. (A) Scheme of *mpeW* interruption and PCR verification of non-complemented and complemented *mpeW* mutant. (B) Scheme of *mpeQ* interruption and PCR verification of non-complemented and complemented mutant *mpeQ* mutant.

SI References:

1. G. K. Farrant, *et al.*, Delineating ecologically significant taxonomic units from global patterns of marine picocyanobacteria. *Proc. Natl. Acad. Sci.*, 201524865 (2016).
2. J. E. Sanfilippo, *et al.*, Interplay between differentially expressed enzymes contributes to light color acclimation in marine *Synechococcus*. *Proc. Natl. Acad. Sci.* **116**, 6457–6462 (2019).
3. A. Shukla, *et al.*, Phycoerythrin-specific bilin lyase-isomerase controls blue-green chromatic acclimation in marine *Synechococcus*. *Proc. Natl. Acad. Sci.* **109**, 20136–20141 (2012).
4. C. Six, *et al.*, Diversity and evolution of phycobilisomes in marine *Synechococcus* spp.: a comparative genomics study. *Genome Biol* **8**, R259 (2007)